7-1

SECURITY INFORMATION

[redacted]

Copy 252
RM L52J02

NACA RM L52J02

7371

[redacted]

NACA

RESEARCH MEMORANDUM

PRELIMINARY INVESTIGATION OF A RECTANGULAR SUPERSONIC SCOOP INLET WITH SWEPT SIDES DESIGNED FOR LOW DRAG AT A MACH NUMBER OF 2.7

By Raymond J. Comenzo and Ernest A. Mackley

Langley Aeronautical Laboratory
Langley Field, Va.

NATIONAL ADVISORY COMMITTEE
FOR AERONAUTICS

WASHINGTON
November 26, 1952

319.98/59

[redacted]

[redacted]

NATIONAL ADVISORY COMMITTEE FOR AERONAUTICS

RESEARCH MEMORANDUM

PRELIMINARY INVESTIGATION OF A RECTANGULAR SUPERSONIC SCOOP INLET WITH SWEPT SIDES DESIGNED FOR LOW DRAG AT A MACH NUMBER OF 2.7

By Raymond J. Comenzo and Ernest A. Mackley

SUMMARY

A preliminary investigation of a swept, rectangular, supersonic scoop inlet designed to have low external drag at the design Mach number of 2.7 has been conducted at the Langley Aeronautical Laboratory. The inlet was tested with two simulated fuselages having circular and rectangular cross sections. Various methods of boundary-layer removal were employed with the rectangular-fuselage configuration. Pressure-recovery and mass-flow data are presented for angles of attack of -5°, 0°, and 5° at Mach numbers of 2.03 and 2.71. A few results were obtained at a Mach number of 3.12 for the simulated fuselage of circular cross section.

The maximum values of total-pressure recovery attained at an angle of attack of 0° were 0.90, 0.77, and 0.58 for free-stream Mach numbers of 2.03, 2.71, and 3.12, respectively, with corresponding mass-flow ratios of 0.60, 0.92, and 1.0. The point of maximum total-pressure recovery also corresponded to the point just before the onset of "buzz" or unsteady flow and, because of this instability, no variation in mass flow is possible near maximum pressure recovery. A means of variable geometry, a triangular "pie-shaped" wedge, was installed in an attempt to obtain a variation in mass flow while maintaining a high pressure recovery. In general, deflection of the wedge delayed the onset of buzz to a lower value of entering mass flow at the expense of a small reduction in pressure recovery. Boundary-layer suction gave almost no change in total-pressure recovery at Mach number 2.03 and an increase in total-pressure recovery of approximately 8 percent at Mach number 2.71. Mach number distributions in the subsonic diffuser are also presented.

INTRODUCTION

The primary object of supersonic inlets for air-consuming engines is to decelerate the air from supersonic to subsonic Mach numbers with high pressure recovery and low drag. Various methods of obtaining high pressure recovery and low drag have been utilized with good results in the range of Mach numbers below approximately two. In reference 1, an inlet having all-internal supersonic compression was presented, and the criteria for the "starting" process of simple convergent-divergent supersonic inlets was discussed. A different approach to the design of supersonic inlets was introduced in reference 2, revealing the beneficial effects of external compression on the inlet starting and operating characteristics. A modification to the convergent-divergent inlet, consisting of perforations about the circumference of the inlet and incorporating a contraction ratio greater than the limiting value given in reference 1, is presented in reference 3.

In 1944, Oswatitsch (ref. 4) considered the possibility of air-consuming engines as a means of propulsion at higher Mach numbers and designed an inlet for a Mach number of 2.9. A theoretical analysis is presented (ref. 4) in which Oswatitsch recognized the inlet-starting limitations due to the required contraction ratio and also the importance of external compression to obtain high values of pressure recovery. The double-spiked Oswatitsch inlet was tested at a Mach number of 2.9, and a high value of pressure recovery was obtained with moderate drag.

At a later date, Ferri and Nucci (ref. 5) made comprehensive theoretical and experimental analyses on the single-cone inlet (commonly called Ferri type). Numerous variations of cone angle, cowl design, and internal contractions were tested at Mach numbers of 2.45, 2.75, and 3.30. In reference 5, the difficulties associated with the design of a conical inlet for these Mach numbers in comparison to lower Mach numbers is thoroughly discussed. In order to attain high values of pressure recovery at Mach numbers above 2.4, the drag of conical inlet designs appears excessive. This high drag is primarily caused by the large cowl-lip angles required which result in high pressures on the external surface of the cowl.

The rectangular scoop inlet for a Mach number of 2.7 discussed herein was designed to have a value of pressure recovery comparable to conical inlets but with much lower drag. A similar type inlet designed for a Mach number of 1.9 was presented in reference 6. The configuration tested in reference 6 was not completely started and, therefore, the maximum value of pressure recovery obtained was much lower than that of the conical inlet tested in reference 2. Dr. Antonio Ferri designed the inlet described herein and initiated the present investigation.

The purpose of this investigation was to determine the characteristics of this rectangular scoop inlet designed for a Mach number of 2.7. The data include total-pressure recovery, mass flow, and shadow photographs for Mach numbers of 2.03, 2.71, and 3.12 at angles of attack of $\pm 5^{\circ}$ and 0°.

SYMBOLS

M_o	free-stream Mach number
M_1	subsonic-diffuser exit Mach number
$\frac{P}{P_o}$	ratio of total pressure at exit of subsonic diffuser to free-stream total pressure (the pressure-recovery ratio was calculated on a weighted mass-flow basis)
$\frac{m_m}{m_o}$	ratio of measured mass flow to mass flow through a free-stream tube of cross-sectional area equal to the inlet frontal area at the Mach number considered (the free-stream-tube area does not include the frontal area of the boundary-layer bleed for the offset fuselage configuration)
$\frac{m_b}{m_m}$	ratio of the measured mass flow through the boundary-layer bleed-off slot to the measured mass flow through the inlet
C_{L_w}	pressure lift coefficient of wedge based on the inlet frontal area
α	angle of attack
δ_w	wedge deflection or wedge angle
R	Reynolds number

INLET AERODYNAMIC DESIGN

Drag.- Consider first a two-dimensional nose inlet having high external compression with a shock pattern as shown in figure 1(a). This type inlet can have a high pressure recovery and will have high drag because of the required large cowl-lip angle. Replace the streamline a-a that wets the surface of the cowl with a solid boundary which can be considered to represent a fuselage (fig. 1(b)). A scoop inlet is thus formed having the same internal aerodynamic design as the nose inlet (fig. 1(a)) but with much lower drag, since the external shock caused by the cowl lip no longer exists. This scoop inlet will retain the high-pressure-recovery characteristics of the nose inlet but with much lower drag provided the inlet will start with the contraction ratio required in the design condition and the adverse effects of the fuselage boundary layer are eliminated by suction or other means.

Starting phenomena.- A critical part of the operation of this type of inlet is the starting process. The inlet is considered completely started in the design condition, in which the first shock wave from the compression surface lies just inside the side walls all the way to the upper lip with a mass-flow ratio m_m/m_o of unity. Starting infinite two-dimensional and axially symmetric inlets having external compression is accomplished by means of the spillage around the cowl which allows the frontal shock to move to the cowl lip in the starting process (fig. 2(a)). If the side walls of the two-dimensional scoop inlet (fig. 1(b)) were closed at AB, it would operate as a simple convergent-divergent diffuser; however, the contraction ratio associated with this type design would be higher than the limiting value given in reference 1, and, therefore, the inlet would not start. If the side walls were swept back along the line AC, (as indicated in fig. 1(b)), the starting phenomena would be different and can be qualitatively discussed with the aid of figure 2(b). Since the fuselage now is in a position corresponding to that of the cowl lip in infinite two-dimensional and conical inlets, spillage does not occur over a similar lip; however, spillage can occur laterally or out the sides, since the inlet has a finite width. Consider a section LM (fig. 2(b)) for a given position of the normal shock P. The leading edges of the sides of the inlet NN are far from the shock; hence, spillage can occur out the sides so that the inlet can start. The amount of spillage is a function of the width and height of the inlet, sweepback of the side walls, and shape of the fuselage. For a given design Mach number, decreasing the width of the inlet makes the starting problem easier. An approximate theoretical analysis of the starting phenomena is difficult; therefore, an experimental investigation has been initiated with the inlet presented herein being the first of a series to be tested.

Internal design.- The inlet design for a Mach number of 2.7 consisted of an initial angle of 14° and a total deviation of 28° obtained by gradual compression. (See fig. 3.) The initial angle of 14° was selected as a reasonable value from the viewpoint of theoretical pressure recovery. The Mach number behind the last isentropic compression wave was approximately 1.6. This Mach number was chosen fairly high to allow for the uncertainties of the effect of boundary layer on the starting phenomena. The initial shock wave and the isentropic compression waves were made to coalesce at point B (fig. 3). The upper surface was then turned in the direction of the flow, and a relatively long minimum section was used for normal-shock stabilization. The subsonic diffuser had a divergence angle of 8° between the upper and lower surfaces with the width of the duct being constant.

Variable geometry.- Initial tests indicated that subcritical operation at the Mach numbers tested was not possible; that is, almost no variation of mass flow with increasing back pressure was possible at $M_o = 2.03$ and $M_o = 2.71$ because of flow instability or buzz phenomena. Hence, a method of variable geometry was incorporated for the purpose of obtaining some variation in mass flow. The variable-geometry scheme consisted of a "pie-shaped" triangular wedge (fig. 4) located in the simulated fuselages. An angle of approximately 34° was chosen for the apex of the wedge to assure shock attachment at $M = 2.0$. A triangular shape was used primarily because of drag considerations and the possibility of diverting the boundary layer of the fuselage around the sides of the inlet.

MODEL AND TESTS

The investigation was performed in blowdown jets of the Gas Dynamics Branch by using low-humidity air from large pressurized tanks. The test sections used for each Mach number and corresponding Reynolds numbers are shown in the following table:

M	Test section	R, per inch
2.03	6 × 7 open	2.03×10^{6}
2.71	6 × 5 closed	2.21×10^{6}
3.12	9 × 8 closed	2.41×10^{6}

Model.- The model was constructed in two parts, inlet and simulated fuselage. This was done in order that the fuselage cross section could be changed from rectangular to circular in front of the inlet (figs. 4 and 5). A pie-shaped triangular-shaped wedge was placed in the rectangular fuselage pivoting about point A (fig. 6) and thus projected the apex into the air stream a certain height B. This height, (that is, the wedge angle) was varied for the tests. In the case of the circular fuselage, wedges of three different heights at the apex were placed separately on the fuselage giving approximately the same effect as the movable wedge in the rectangular fuselage. Static-pressure orifices were placed in the exposed surface of the wedge used in the rectangular fuselage (fig. 7). These measurements were made to obtain some indication of the loads to be expected on the wedge.

<u>Tests</u>.- Tests were run at three different angles of attack (±5° and 0°) with the entire model and piping hinging about point C (fig. 6). The portion of the tunnel boundary layer in front of the scoop was removed by the forward portion of the simulated fuselages for both rectangular and circular section, as indicated in figures 4 and 5. Because of the spillage around the circular-fuselage configuration tested, no other provision was made for the removal of the boundary layer on the circular fuselage in front of the inlet; however, the following tests were made with the rectangular-fuselage configuration:

1. Fuselage boundary layer removed by means of a "bleed-off slot" located just ahead of the point of shock convergence (fig. 4(a)) with suction being applied. This configuration is referred to as the flush-fuselage condition.

2. The bleed-off slot sealed, with the fuselage condition stated in 1 above so that there is no boundary-layer removal except that possibly caused by the deflection of the wedge.

3. The fuselage section moved upward relative to the inlet (fig. 4(b)) and the "slot" open. Tests were run with suction applied and the bleed-off slot open to atmospheric pressure. The static pressure in front of the bleed-off slot was greater than atmospheric for $M = 2.03$ and lower than atmospheric for $M = 2.71$. This configuration is referred to as the offset fuselage condition.

<u>Measurements</u>.- The total and static pressures were measured in the subsonic diffuser, and the mass flow through the model was measured by a calibrated orifice located between the pressure-measuring station and the throttling valves (fig. 6). The total temperature was also measured near the orifice. The pressures at the rake and orifice were indicated on gages, and a mercury-filled "U" tube was used to measure the differential across the orifice; whereas the pressures at the small orifices in the wedge were indicated on mercury manometer boards. The mass flow through the bleed-off slot was measured by means of a venturi when suction was applied. All readings were recorded photographically. The pressure measurements taken are estimated to be accurate within 1 percent and give pressure recovery (which was obtained on a weighted mass-flow basis) and mass-flow ratio values accurate to ±2 percent.

ANALYSIS AND DISCUSSION

<u>Shadow photographs</u>.- Shadow photographs of all configurations investigated are presented in figures 8 to 13. Whenever possible, reference will be made to the shadow photographs in order to explain the phenomena

in the analysis of the data. The disturbances labeled (a) and (b) on figure 8(b) are due to a poor junction between the glass and side walls and exist only along the side walls of the tunnel. They are also noticeable in figure 9(a) for $M = 2.03$. Disturbances labeled (c) and (d) (fig. 8(b)) originate from the forward portion of the simulated fuselage and the junction between the fuselage and nozzle block, respectively. In all other shadow photographs the disturbance from the forward portion of the simulated fuselage exists for all configurations and Mach numbers investigated. This disturbance, a portion of which enters the inlet, is believed to have a negligible effect on the inlet characteristics.

Pressure recovery.- Figure 14 presents the maximum pressure-recovery values at 0° and $\pm 5^{\circ}$ angles of attack for the Mach numbers indicated. A point of prime importance is the fact that the maximum total-pressure recovery is obtained just prior to the onset of buzz or unsteady flow. Thus, when operating at maximum pressure recovery a small reduction in entering mass flow (that is, an increase in back pressure) could cause a sudden and much larger decrease in entering mass flow with a corresponding large increase in drag. The experimental points are connected by a continuous curve; however, this curve may not be strictly correct since the flow phenomena may induce instability or unsteady flow, or separation may occur differently at Mach numbers other than those tested. In the discussion, however, it is assumed that the inlet operation is steady and continuous through the Mach number range. From figure 14 it can be seen that the pressure recovery is lower for the -5° angle of attack than for either 0° or 5° angles of attack, except for the offset configuration operating at $M_o = 2.71$ with the bleed-off slot open to atmospheric pressure. The lower pressure recovery that exists at an angle of attack of -5° for most of the configurations tested at $M_o = 2.71$ and 2.03 (fig. 14) is primarily due to the separation that exists on the fuselage ahead of the inlet as shown by the shadow photographs in figures 8 and 9. A low-pressure region is present on the surface of the fuselage at this angle of attack, and the boundary-layer air tends to accumulate in this region. In addition, the high pressure gradient (due to the coalesced compression waves) aggravates this condition and induces separation.

A possible improvement that can be applied to the original design is that of allowing the compression waves to be spread out as indicated on figure 15 in contrast to having them coalesce as shown on figure 3. This change might tend to reduce the flow separation and tend to improve the operation at Mach numbers above 2.7. The compression waves at $M_o = 3.0$ will become more oblique than shown on figure 3 but will not coalesce downstream of the inside duct surface (fig. 16); hence, less expansion is required around the corner. The internal contraction, however, limits the amount that the compression waves can be spread out because of increased difficulties in the starting process.

From the shadow photographs of figure 11(b) at the design Mach number of 2.71, it can be seen that the inlet is not completely started in the offset configuration; however, this condition appears to have a negligible effect on the pressure recovery. The failure of the inlet to start completely is believed to be due to the bleed-off slot being of poor design (the shape of the slot (fig. 4) was determined by the model structure and not by aerodynamic design). As a result, the deviation required of the flow entering the slot was excessive.

In the offset configuration with the bleed-off slot open to atmospheric pressure the pressure recovery at Mach number 2.71 is higher for -5° angle of attack than either 0° or 5° angle-of-attack conditions. The Mach number on the surface of the fuselage is higher for $\alpha = -5^{\circ}$ than for $\alpha = 0^{\circ}$ or 5°. The detached shock wave occurs ahead of the inlet upper lip as a result of the total flow deviation required and has a lesser effect on the inlet pressure recovery at $\alpha = -5^{\circ}$ because less of the low-energy air behind the detached shock wave enters the inlet.

A point of interest is the vortex sheet that is present due to the intersection of the shock from the compression surface with the shock ahead of the upper lip of the inlet (designated (a) in fig. 11(b)). This vortex sheet is visible for $\alpha = 0^{\circ}$ and -5°, but not very clear for $\alpha = 5^{\circ}$. The direction of the vortex sheet is in toward the bleed-off slot so that the pressure at this point is greater than atmospheric and the air is flowing away from the inlet and into the bleed-off slot.

In the design condition, $M_o = 2.71$ and $\alpha = 0^{\circ}$, the circular-fuselage configuration attained a pressure recovery of 0.77 (fig. 14), which was the maximum value of all configurations tested. The lowest value of pressure recovery $\left(\frac{P_o'}{P_o} = 0.725\right)$ was obtained for the rectangular fuselage with the bleed-off slot sealed. The pressure recoveries for all other configurations tested at $M_o = 2.71$ and $\alpha = 0$ lie between the values quoted and are indicated in figure 14. The effect of angle of attack at $M_o = 2.71$ was to decrease the maximum value of pressure recovery approximately 5 percent.

At $M_o = 2.03$ and $\alpha = 0^{\circ}$ (fig. 14), the maximum and minimum values of pressure recovery obtained were 0.90 and 0.86 for the offset fuselage and flush fuselage with bleed-off slot sealed, respectively. The effect of angle of attack on pressure recovery was negligible for $\alpha = 5^{\circ}$ and decreased the value of pressure recovery approximately 8 percent for $\alpha = -5^{\circ}$.

Only the circular-fuselage configuration was tested at $M_o = 3.12$ since it produced higher values of pressure recovery in the design condition, $\alpha = 0^{\circ}$ and $M_o = 2.71$, than any of the other configurations tested. The circular-fuselage configuration tested had good starting characteristics because air of a static pressure slightly higher than free stream readily spilled around the fuselage. The fairing of this fuselage with the inlet side walls (the side walls become tangent at the maximum diameter of the fuselage in front of the inlet) can be seen in the photograph of figure 5(a). The fairing is important at $M_o = 2.71$ because the fuselage boundary-layer spillage that occurs helps to prevent separation near the upper lip.

With the inlet operating at $M_o = 3.12$, the free-stream Mach number is further increased by the presence of an expansion about point B (shown in fig. 16); therefore, the losses incurred across the normal shock are large. It is believed that some separation exists in the diffuser which effectively causes some internal contraction and the pressure recovery is aided slightly in this condition of operation.

Figure 17 compares the values of pressure recovery at $\alpha = 0$ for the circular- and flush-fuselage configurations with that of a conical inlet designed for each respective Mach number where a symbol is indicated. The pressure recovery of the inlet tested herein is approximately the same as that of the best conical inlets from $M_o = 2.0$ to 2.5 (refs. 2 and 5) and slightly higher from $M_o = 2.5$ to 3.0. Above $M_o = 3.0$ no direct comparison can be made, but it may be safe to say that the pressure recovery of this particular inlet will be lower than that of the best conical types. Inlets designed by the criteria presented herein for a Mach number above 3.0, however, should attain pressure-recovery values equal to or above that possible for conical-type inlets of the same design Mach number and have lower drag in the design condition.

Wedge effects.- For all configurations discussed, the entering mass flow cannot be varied from that for which maximum pressure recovery is obtained because of the instability or buzz phenomena that is encountered. Variation of mass flow may be necessary in both the design and off-design conditions in order that the inlet might efficiently meet the air requirements of the engine. Since the pressure-recovery characteristics of this inlet appeared promising, a method of variable geometry was installed in an attempt to improve the operation of the inlet through a range of Mach numbers.

When the wedge is projected into the stream in a small amount, the air stream in front of the inlet and next to the fuselage is deflected by the sides of the wedge with accompanying oblique shock waves. The deflected air at increased static pressure flows upward to the low-pressure region on the vertical sides of the fuselage and the inlet entering mass flow then is decreased. As the apex of wedge is projected into the stream further, however, the static pressure on the bottom of the wedge becomes lower and air at a higher static pressure on the sides of the wedge flows down into this low-pressure region as well as outward and upward. Although more of the free-stream tube is deflected outward at the apex of the wedge, the effectiveness at a large δ_w is decreased.

The effect of wedge deflection on the pressure recovery and mass-flow ratio at $M_o = 2.03$ is shown in figure 18. Generally, the deflection of the wedge has a negligible effect on the pressure recovery for all configurations tested at $\alpha = 0^\circ$, $\alpha = -5^\circ$, and the circular and rectangular fuselage with bleed-off slot sealed at $\alpha = 5^\circ$. The pressure recovery increases, as shown in figure 18, for wedge angles up to about 6° and then decreases for wedge angles above 6°.

In some instances, at $M_o = 2.03$, the deflection of the wedge has an appreciable effect on the inlet entering mass flow as evidenced by the data in figure 18. The discussion of this variation and the corresponding effect on pressure recovery may be clarified with the aid of figure 19. The points on the solid portion of the curves correspond to the maximum values of pressure recovery attainable for each configuration. The back pressure is increased (as indicated by the dotted lines for $\delta_w = 0^\circ$, figs. 19 and 21) until the point of maximum pressure recovery is obtained which also corresponds to the condition precisely before the onset of buzz or unsteady flow.

Mass-flow and pressure-recovery characteristics of the circular-fuselage configuration (fig. 19(a)) for $M_o = 2.03$ are unaffected by wedge deflection at all angles of attack tested. The reason for the wedge being ineffective for this configuration is believed to be that the wedge is completely immersed in the separated region, as shown in the shadow photographs of figure 12. In contrast, for other configurations tested the wedge apex is slightly forward of the separated region (fig. 13). Should the apex of the wedge be placed farther forward of the separated region, it is believed that its effect on the mass flow entering the inlet would be more pronounced.

For the rectangular-fuselage configurations the general effect of increasing the wedge deflection is to decrease the mass flow and pressure recovery a small amount (fig. 19). At $\alpha = 5^\circ$ the effectiveness of the wedge in varying the mass flow is improved over $\alpha = 0^\circ$ but with increased loss in pressure recovery; at $\alpha = -5^\circ$ the wedge is less effective in varying the mass flow than at $\alpha = 0^\circ$ with less loss in pressure recovery.

For $M_o = 2.71$ the effect of an increase in wedge deflection is to decrease the pressure recovery and mass-flow ratio of the inlet at all angles of attack investigated (fig. 20). The correlated variation of pressure recovery with mass flow for a change in wedge deflection can best be seen on figure 21. Figure 21 also shows angle of attack has less effect on the mass flow and pressure recovery at $M_o = 2.71$ than at $M_o = 2.03$ and that the variation of mass flow with wedge angle is nonlinear.

The comparative changes in mass-flow ratio and total-pressure recovery from $\delta_w = 0^\circ$ to the maximum wedge deflection tested $\left(\delta_{w_{max}}\right)$ for $M_o = 2.03$ and $M_o = 2.71$ are compiled in the following table for all angles of attack and configurations tested:

Configuration	α, deg	$M_o = 2.03$			$M_o = 2.71$		
		$\Delta \frac{m_m}{m_o}$	$\Delta \frac{P}{P_o}$	$\delta_{w_{max}}$	$\Delta \frac{m_m}{m_o}$	$\Delta \frac{P}{P_o}$	$\delta_{w_{max}}$
Circular fuselage	-5	0.000	-0.010	13°30'	-0.080	-0.020	13°30'
	0	.000	-.015	13°30'	-.180	-.100	13°30'
	5	-.003	-.002	13°30'	-.190	-.090	13°30'
Flush fuselage "bleed-off" slot sealed	-5	.000	.000	15°30'	-.110	-.050	15°30'
	0	-.055	-.010	15°30'	-.140	-.120	15°30'
	5	-.055	-.000	15°30'	-.170	-.100	15°30'
Flush fuselage suction applied	-5	-.050	-.010	15°30'	-.200	-.065	17°
	0	-.130	-.022	16°30'	-.160	-.120	17°
	5	-.120	-.050	16°30'	-.110	-.055	15°30'
Offset fuselage suction applied	-5	-.002	.000	16°	-.095	-.060	16°30'
	0	-.045	.003	16°	-.040	-.040	16°45'
	5	-.110	-.025	17°	-.040	-.020	16°30'
Offset fuselage "bleed-off" slot open to atmospheric pressure	-5	-.045	.000	16°30'	-.110	-.060	16°45'
	0	-.070	-.015	16°	-.135	-.050	17°30'
	5	-.090	-.032	16°30'	-.065	-.035	17°30'

where the prefix Δ indicates the change caused by increasing the wedge deflection from $\delta_w = 0^\circ$ to $\delta_{w_{max}}$ and the negative sign indicates a lower value than that attained at $\delta_w = 0^\circ$.

The wedge effects discussed previously above are for a specific wedge and can not be considered to apply generally because the geometry and placement of the wedge are important to the effectiveness in reducing the mass flow and keeping the pressure recovery high. Generally, the apex of the wedge should be ahead of the point where boundary-layer separation occurs for $\delta_w = 0^{\circ}$ and should have a small angle for shock-wave attachment and low drag.

Drag.- Although the drag of the inlet was not measured in this investigation, the inlet was designed so that at the design Mach number and angle of attack the initial shock wave from the compression surface should be just inside the inlet side walls. The external shock waves and resulting drag would thus be reduced to a minimum and the design mass-flow ratio would be unity (that is, no spillage). In this investigation, however, spillage (shown by values of m_m/m_o in fig. 21) was present because of varying amounts of separation near the upper lip of the inlet and the first shock wave from the compression surface being slightly in front of the inlet side walls (figs. 8(b) and 9(b)). A reduction in this spillage would reduce the accompanying drag.

At $M_o = 2.03$ the mass-flow ratio is never greater than 0.7 and is approximately 0.6 at the point of maximum pressure recovery (fig. 19) showing a large amount of spillage which would be expected to cause high drag. A possible solution at $M_o = 2.03$ is to vary the geometry by changing the lower lip angle and inlet frontal area.

Boundary-layer control.- The mass of air removed by the boundary-layer bleed-off slot was varied at each Mach number for each angle of attack and wedge deflection. Figure 21 presents the pressure-recovery data as a function of the ratio of the measured mass flow through the bleed-off slot to the measured mass flow through the inlet. This comparison can only be made for the flush-fuselage configuration. As indicated on figure 22(a) for $M_o = 2.03$, suction improved the pressure recovery for $\delta_w = 0^{\circ}$ and $\delta_w = 5^{\circ}$ and had a negligible effect on the higher wedge deflection, whereas a positive angle of attack of 5° increased the improvement and a negative angle of attack of 5° decreased the improvement. Figure 22(b), for $M_o = 2.71$, $\alpha = 0^{\circ}$, $\delta_w = 0^{\circ}$ shows an improvement in pressure recovery up to a relative mass-flow ratio through the bleed-off slot of approximately 0.03 and then no further improvement as the relative mass flow is increased. High values of m_b/m_m caused no apparent decrease in inlet entering mass flow at $M_o = 2.03$; at $M_o = 2.71$ there was no apparent decrease in inlet entering mass flow below m_b/m_m of approximately 0.05.

The minimum amount of suction needed for the maximum improvement in pressure recovery becomes important when boundary-layer control is considered for aircraft. The minimum ratio of the mass flow through the bleed-off slot to the measured mass flow into the inlet for the maximum increase in pressure recovery obtained at $M_o = 2.71$ for all angles of attack and wedge deflections investigated is presented in tabular form:

$M_o = 2.71$			
α, deg	δ_w, deg	$\left(\frac{m_b}{m_m}\right)_{min}$	$\Delta \frac{P}{P_o}$
-5	0	0.062	0.040
-5	4	.083	.045
-5	11	.093	.025
-5	16	.100	.025
0	0	.025	.040
0	3	.025	.050
0	9	.025	.070
0	16	.060	.040
5	0	.023	.020
5	4	.023	.030
5	10	.025	.075
5	15	.042	.065

The parameter $\Delta \frac{P}{P_o}$ is the increase in pressure recovery obtained by using suction with respect to the condition where no suction was applied (that is, the flush-fuselage configuration with the bleed-off slot sealed).

<u>Mach number distribution in diffuser</u>.- Presented in figures 23 and 24 are the Mach number distributions at the center line of the subsonic diffuser (which are generally representative of the distributions across the diffuser) for several of the configurations tested at Mach numbers of 2.03 and 2.71, respectively. Figure 23(a) denotes the circular-fuselage configuration ($M_o = 2.03$) in which the wedge was completely immersed in the separated region that exists on the fuselage, as discussed previously. Although the wedge is located in this region, it appears (fig. 23(a)) that deflecting the wedge effectively moves the separation from the lower to the upper surface and thereby increases the Mach number in the region nearest the compression surface. It appears that the expansion from the apex of the wedge in interacting with the compression surface tends to alleviate the separated flow condition that apparently exists for $\delta_w = 0^\circ$.

In figure 23(b) which represents the flow in the duct for the flush-fuselage configuration with the bleed-off slot sealed, it is noticeable that deflecting the wedge had a pronounced beneficial effect on the flow nearest the upper surface (nearest the wedge) of the inlet and a detrimental effect on the flow nearest the compression surface. This effect is also indicated for the flush-fuselage configuration with suction applied (fig. 23(c)). It is considered probable that vortices emanating from the sides of the wedge alleviate the separated condition in a manner similar to that which would be obtained with vortex generators.

The location of the wedge is different for the rectangular- and circular-fuselage configurations and probably accounts for the contrasting effects on the internal flow of the inlet at $M_o = 2.03$. As shown in the shadow photographs of figure 12, the wedge on the circular fuselage is immersed in a separated region of high turbulence and lower Mach number which tend to prevent the formation of vortices as strong as those generated by the wedge of the rectangular fuselage (fig. 13).

For $M_o = 2.71$, deflection of the wedge had a noticeably beneficial effect on the Mach number distribution for all configurations presented in figure 24. The Mach number nearest the compression surface decreases with increasing wedge deflection. Once again for the rectangular-fuselage configuration, wedge deflection tends to reduce the separated condition of the upper surface (nearest the wedge) of the subsonic diffuser; thus reduction in separation is believed to be due to the existence of the vortices as discussed previously.

Wedge loads.- The lift coefficient of the wedge as a function of wedge deflection is presented in figure 25. These measurements were made primarily to obtain some idea of the loads that are to be expected with this type of design.

Aspect-ratio effects.- A parameter of great concern in the inlet design is that of aspect ratio or the height-to-width ratio of the inlet. Fortunately, for the first test configuration a value (1.5) was chosen that proved adequate for starting; however, in most cases the designer would desire an inlet that protrudes from the fuselage a minimum amount. Aspect-ratio values of 1.0 and 0.5 have been quoted as desirable, but the starting process becomes more difficult as the aspect ratio decreases. A method which is considered as a possibility of improving the starting phenomena of low-aspect-ratio inlets is presented in figure 26. The idea involved is to design a bypass system that would allow for some air spillage and hence aid the starting process. The design essentially consists of increasing the entering free-stream-tube area a small amount (say 10 percent) in such a manner that the area of the minimum section is increased about 25 percent. This condition obviously aids the starting process by decreasing the over-all contraction ratio of the inlet. The additional drag of the bypass can be kept low by careful design and the air entering the bypass may be of some use.

<u>Applicability of results</u>.- The boundary layer in front of the upper lip of the inlet is an important factor in the operation of this type inlet. Should this boundary layer on an actual configuration be much different than that of the models tested herein, the results obtained may not be applicable.

For $\pm 5^{\circ}$ angle-of-attack conditions, the Mach number distribution on the model simulated fuselage is undoubtedly quite different from the Mach number distribution of an actual fuselage arrangement. The separation or boundary-layer phenomena encountered at $\alpha = -5^{\circ}$ may be more detrimental in the model tests than would be in actual flight conditions because some of the boundary layer of the nozzle flows into the low-pressure region present on the surface of the fuselage at this angle of attack.

Another point of discussion is that the subsonic-diffuser design of the test model is not practical when applied to an actual configuration, since some turning (see fig. 1) must take place soon after the minimum section. From the present tests it is known that separation exists on the upper and lower surfaces of the inlet and would become more aggravated on the lower surface when the subsonic diffuser is turned in the manner indicated in figure 1. Vortex generators, turning vanes, or surface roughness might reduce the severity of the separated conditions.

The effect of Reynolds number on test results of this type inlet is of prime importance. For the high Reynolds numbers of this investigation given in the section entitled "Model and Tests," a turbulent boundary layer is present on the surface of the fuselage. At low Reynolds numbers where laminar flow exists, however, there is a greater tendency for separation to occur due to pressure rise, such as that which takes place where the compression waves coalesce for the design condition (point B, fig. 3). Therefore, in testing complete models utilizing this type of inlet, the effect of Reynolds number may completely alter the final results.

SUMMARY OF RESULTS

A preliminary investigation has been made of a rectangular supersonic scoop inlet with swept sides designed to have low external drag at $M_o = 2.7$ and $\alpha = 0^{\circ}$. The inlet was tested with simulated fuselages having circular and rectangular cross sections. A pie-shaped wedge which protruded from the surface of the simulated fuselage by varying amounts was investigated as a variable-geometry device in an attempt to obtain some variation of mass flow and to improve the inlet characteristics through a range of Mach numbers. Various methods of boundary-layer removal were employed with the rectangular-fuselage configuration. The following results were obtained from this investigation:

(1) The point of maximum pressure recovery occurred just before the onset of buzz or unsteady flow. The maximum values of total-pressure recovery attained at a wedge deflection of 0° and an angle of attack of 0° were 0.90 at a Mach number of 2.03, 0.77 at a Mach number of 2.71, and 0.58 at a Mach number of 3.12. These pressure-recovery values are higher than the maximum values attained with conical inlets designed for these Mach numbers.

(2) The mass-flow ratios m_m/m_o for the points of maximum pressure recovery given in (1) are 0.60 at a Mach number of 2.03, 0.92 at a Mach number of 2.71, and 1.00 at a Mach number of 3.12. When an attempt is made to reduce these mass-flow ratios by increased back pressure, unsteady flow or buzz phenomena are encountered.

(3) The general effect of angle of attack is to decrease the pressure recovery a small amount.

(4) Deflection of the wedge generally decreases the inlet entering mass flow at the expense of a reduction in total-pressure recovery. The maximum decrease in mass-flow ratio obtained at a Mach number of 2.03 was approximately 0.12 accompanied by a decrease in total-pressure recovery of 0.03; for a Mach number of 2.71 the maximum decrease in mass-flow ratio obtained was approximately 0.16 with a decrease of 0.10 in total-pressure recovery. No variation in inlet entering mass flow was possible without the use of the wedge.

(5) Increasing the relative mass flow entering the bleed-off slot m_b/m_m had a negligible effect on the total-pressure recovery of the inlet at a Mach number of 2.03. At a Mach number of 2.71 a significant effect was measured with an increase in total-pressure recovery of 0.075 being obtained for $\frac{m_b}{m_m} = 0.025$.

(6) The general effect of deflecting the wedge (except for circular fuselage at a Mach number of 2.03) was to shift the separated region within the subsonic diffuser from the upper surface (nearest the wedge)

of the diffuser to the lower surface (continuous with the compression surface) and thereby change the Mach number distribution in the subsonic diffuser.

Langley Aeronautical Laboratory,
National Advisory Committee for Aeronautics,
Langley Field, Va.

REFERENCES

1. Kantrowitz, Arthur, and Donaldson, Coleman duP.: Preliminary Investigation of Supersonic Diffusers. NACA ACR L5D20, 1945.

2. Ferri, Antonio, and Nucci, Louis M.: Preliminary Investigation of a New Type of Supersonic Inlet. NACA TN 2286, 1951.

3. Evvard, John C., and Blakey, John W.: The Use of Perforated Inlets for Efficient Supersonic Diffusion (Revised). NACA RM E51B10, 1951.

4. Oswatitsch, Kl.: Pressure Recovery for Missiles With Reaction Propulsion at High Supersonic Speeds (The Efficiency of Shock Diffusers). NACA TM 1140, 1947.

5. Ferri, Antonio, and Nucci, Louis M.: Theoretical and Experimental Analysis of Low Drag Supersonic Inlets Having a Circular Cross Section and a Central Body at Mach Numbers of 3.30, 2.75, and 2.45. NACA RM L8H13, 1948.

6. Anon.: Survey of Bumblebee Activities. Bumblebee Rep. No. 89, The Johns Hopkins Univ., Appl. Phys. Lab., Oct. 1948.

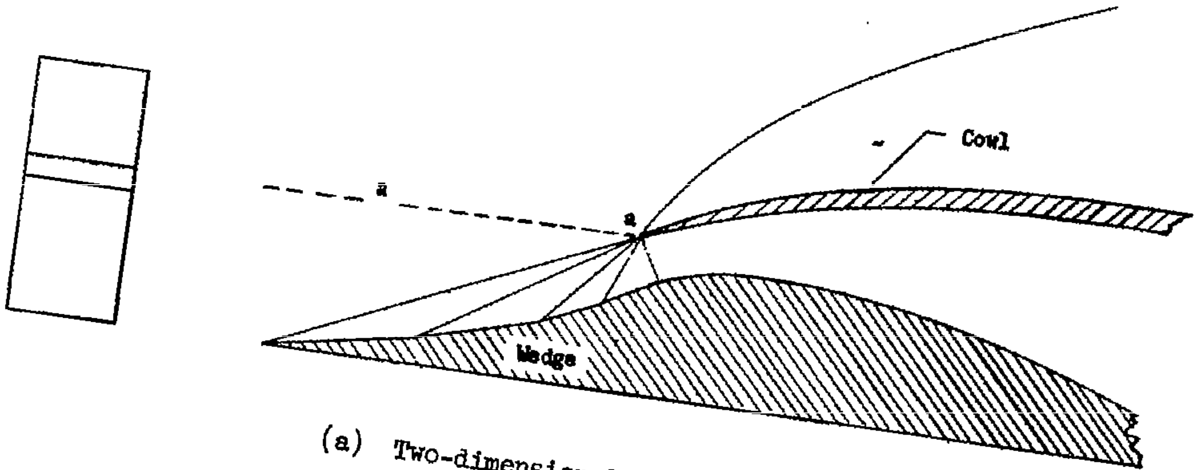

(a) Two-dimensional nose inlet.

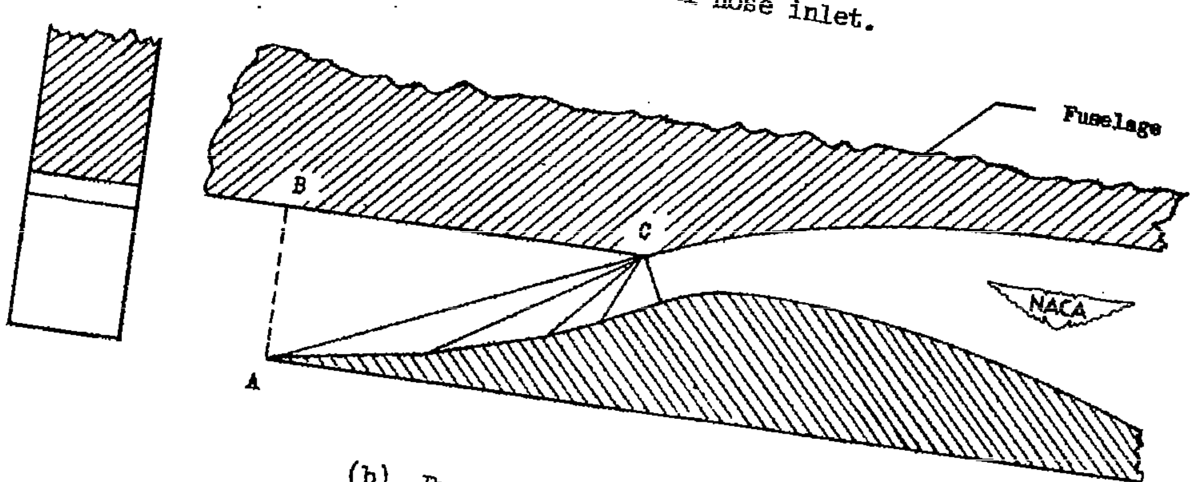

(b) Proposed low-drag inlet.

Figure 1.- Development of a low-drag inlet.

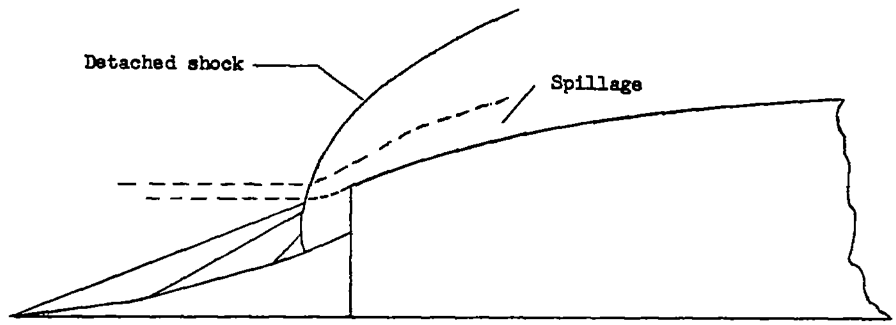

(a) Conical type.

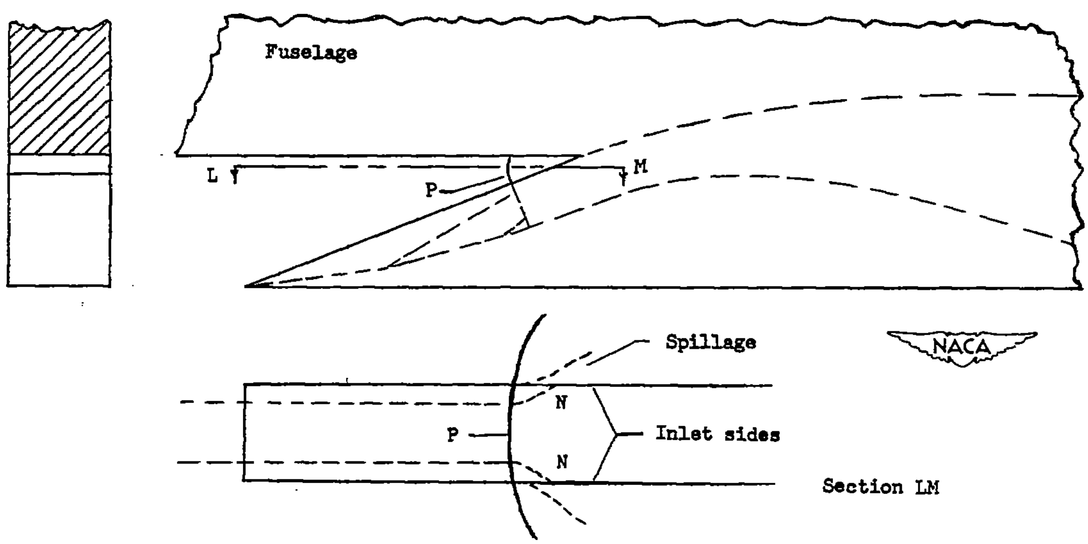

(b) Two-dimensional scoop type.

Figure 2.- Starting phenomena of inlets.

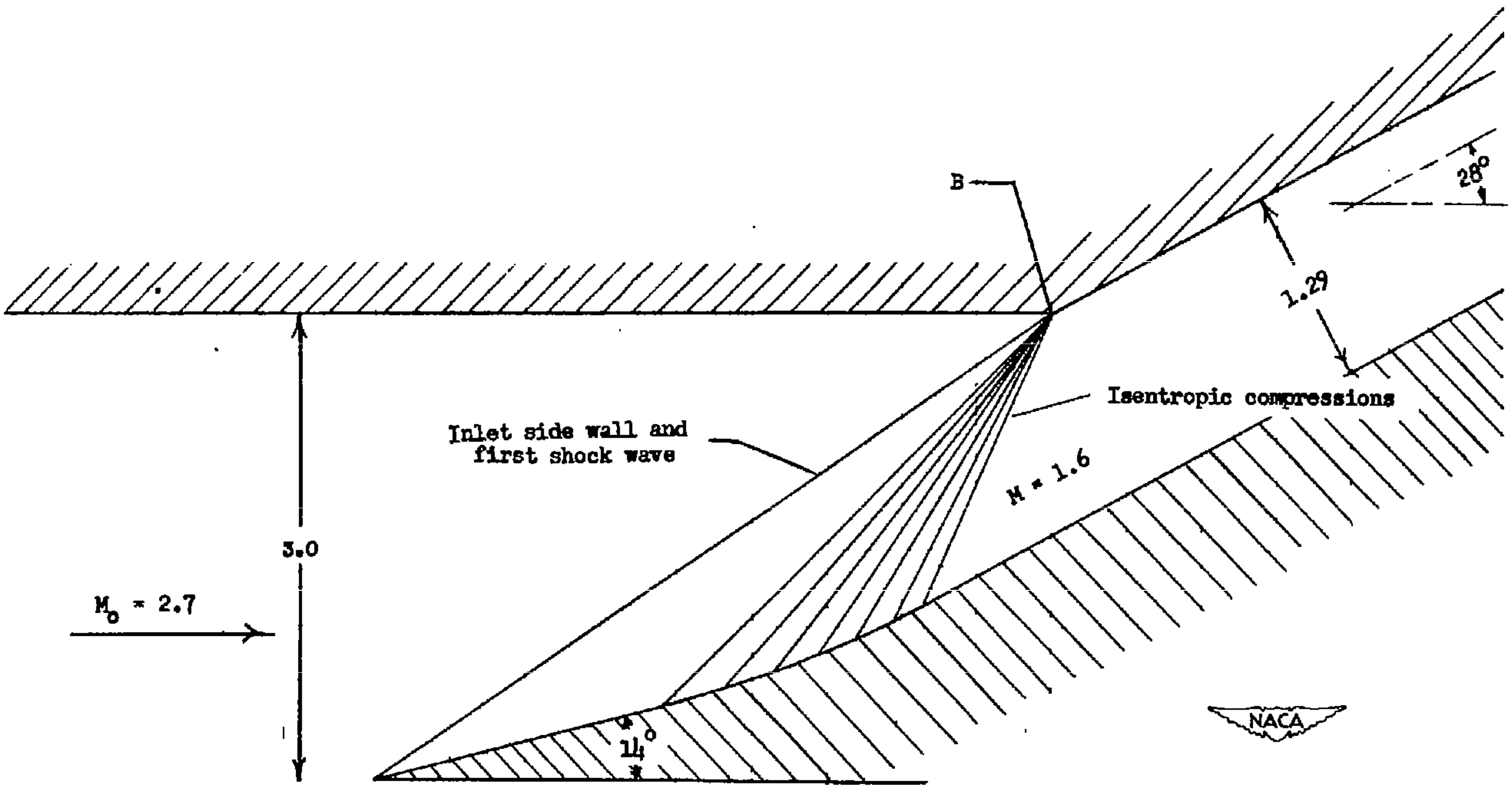

Figure 3.- Design flow pattern for swept, rectangular scoop inlet.

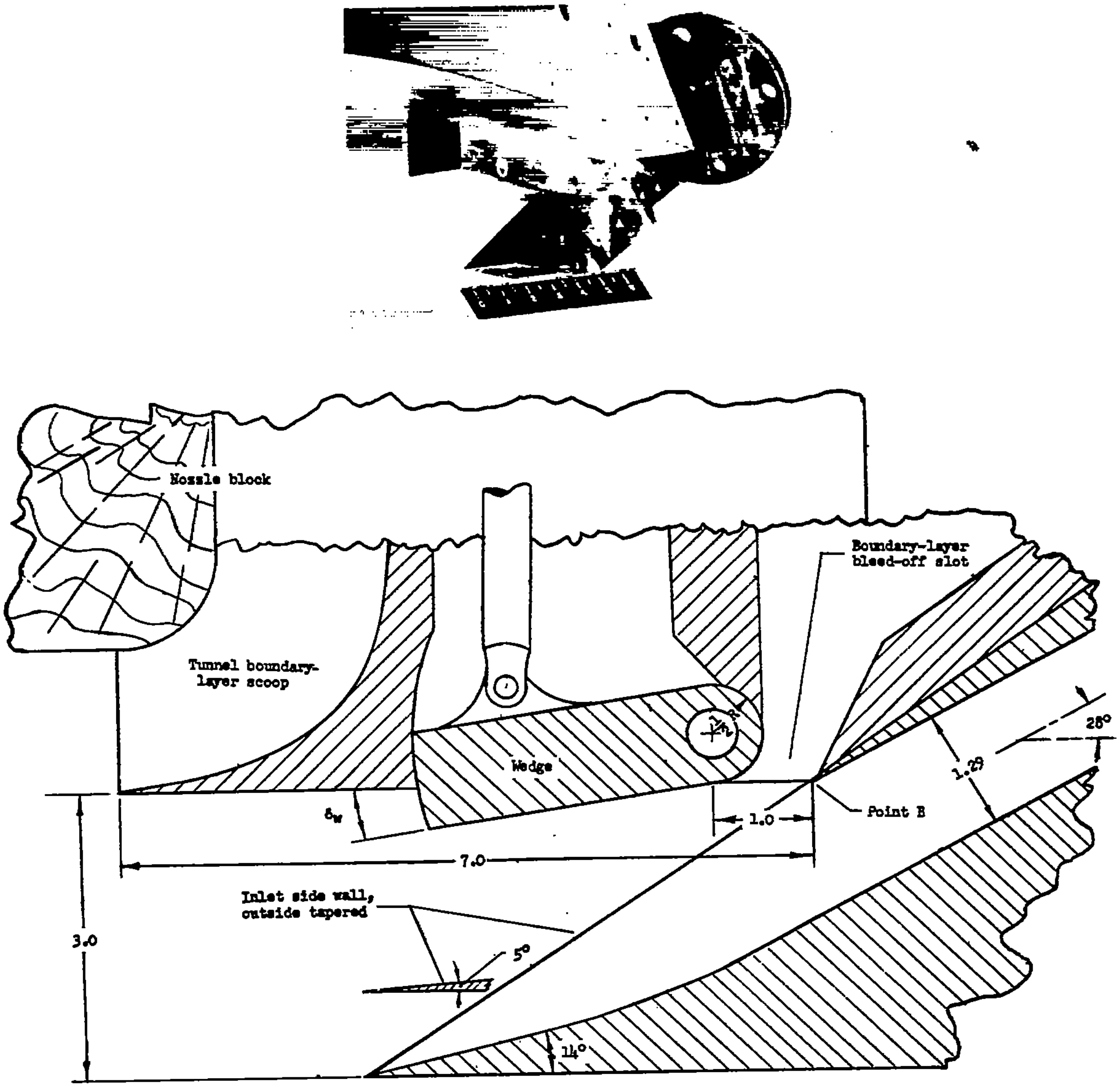

(a) Flush condition.

L-76076

Figure 4.- Details of model with rectangular fuselage.

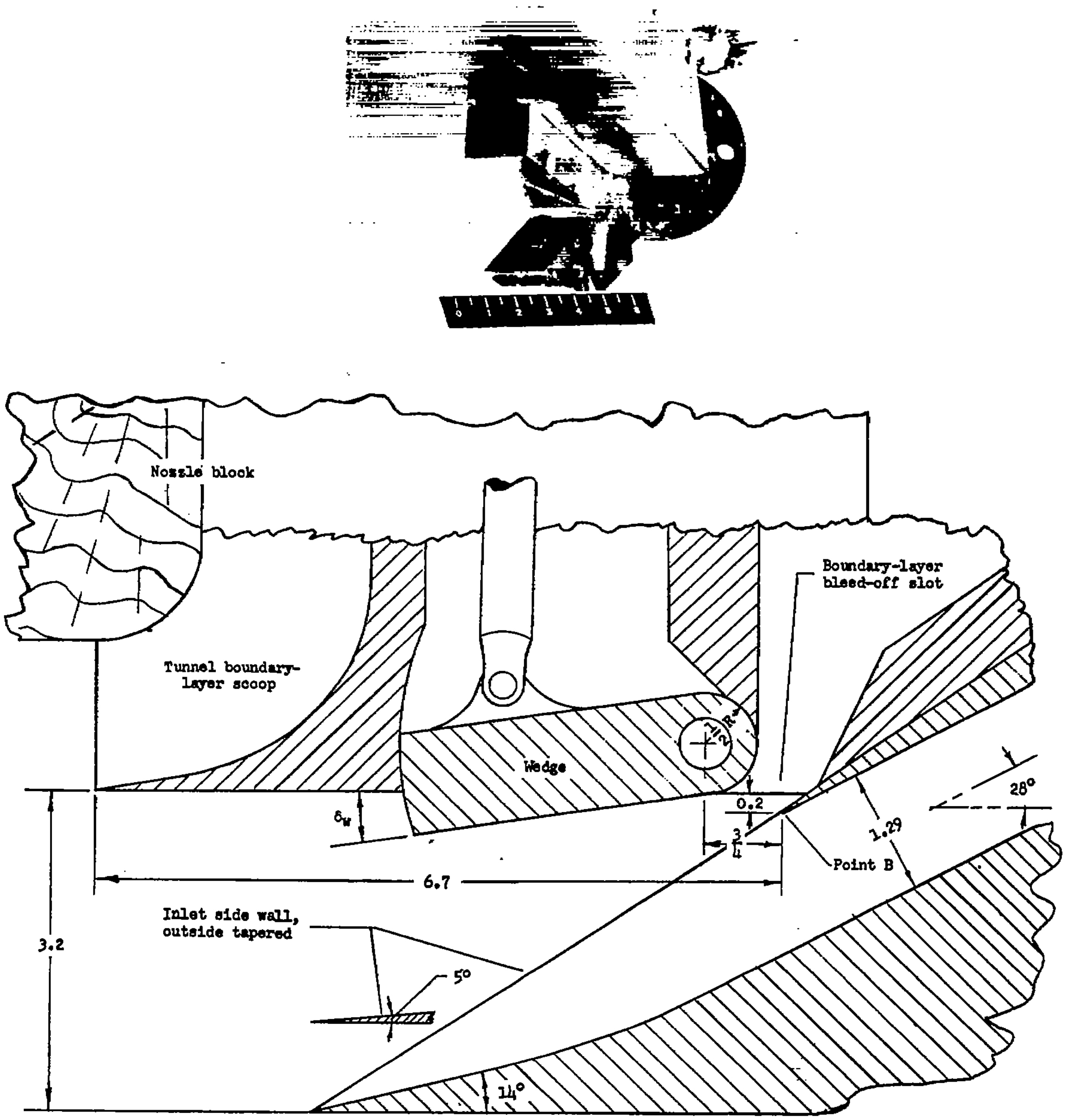

(b) Offset condition.

Figure 4.- Concluded.

L-76077

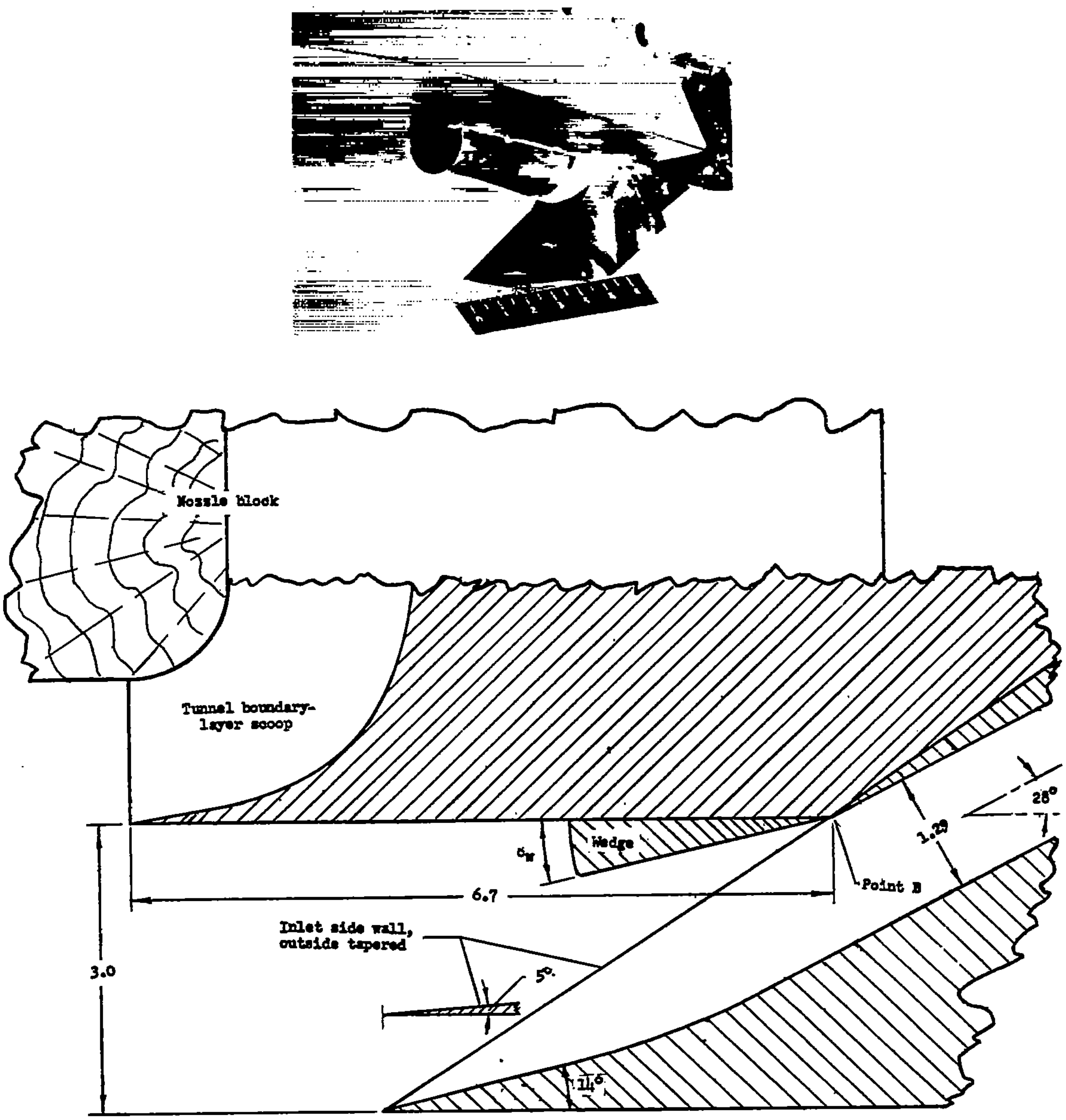

Figure 5.- Details of model with circular fuselage. L-76080

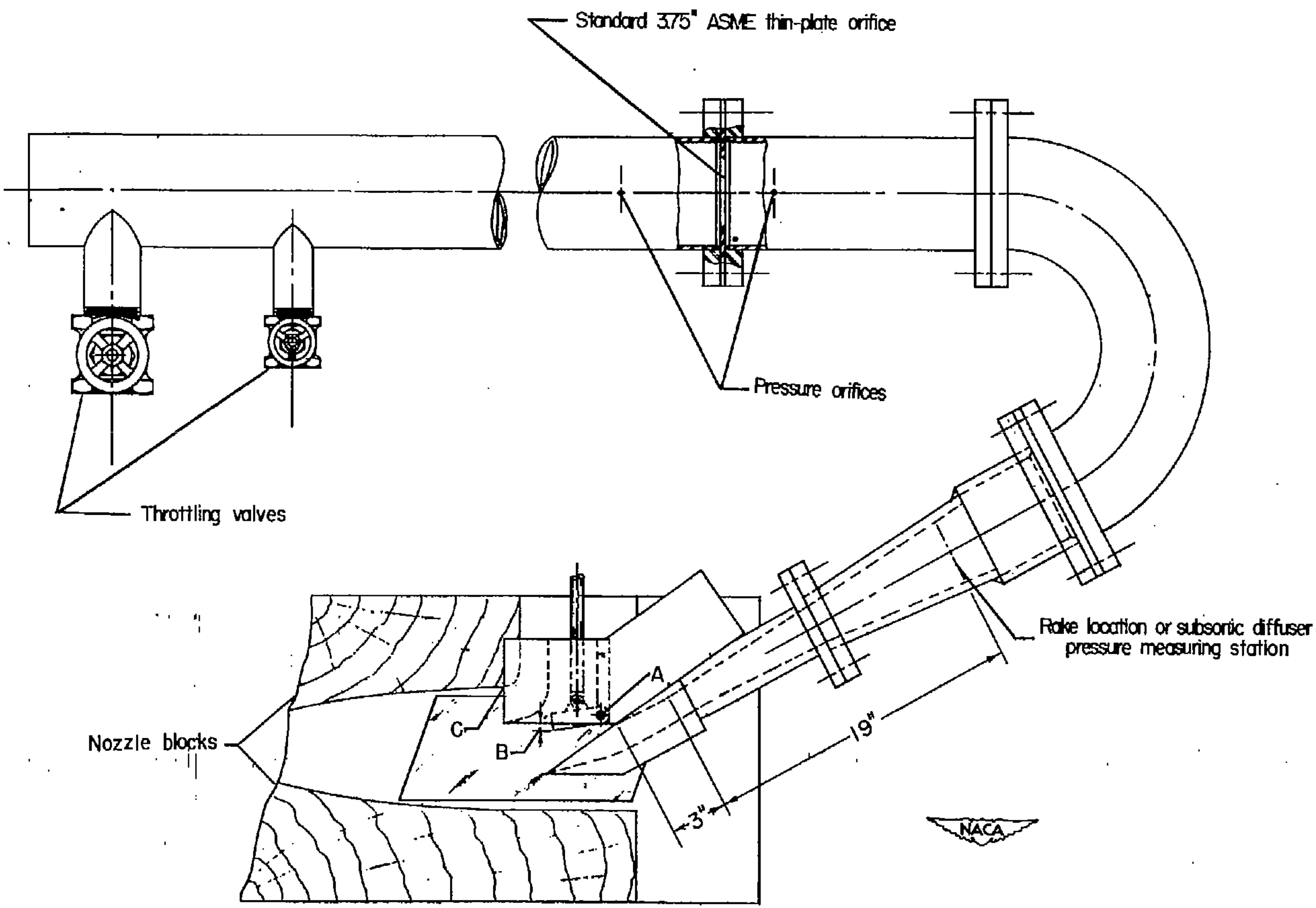

Figure 6.- Schematic drawing of test installation.

[redacted]

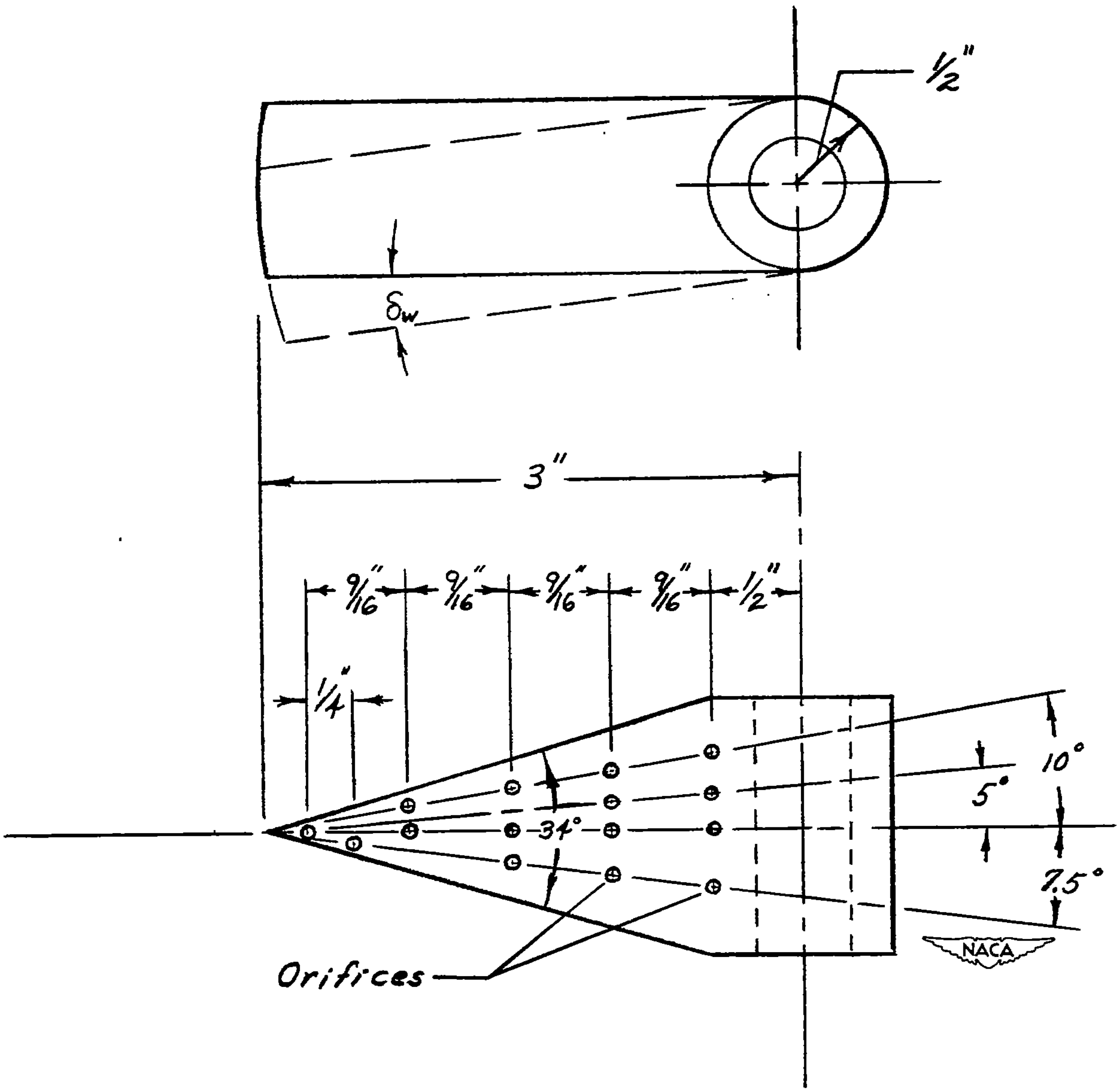

(a) For rectangular fuselage showing static-pressure orifice locations.

Figure 7.- Wedges used in tests.

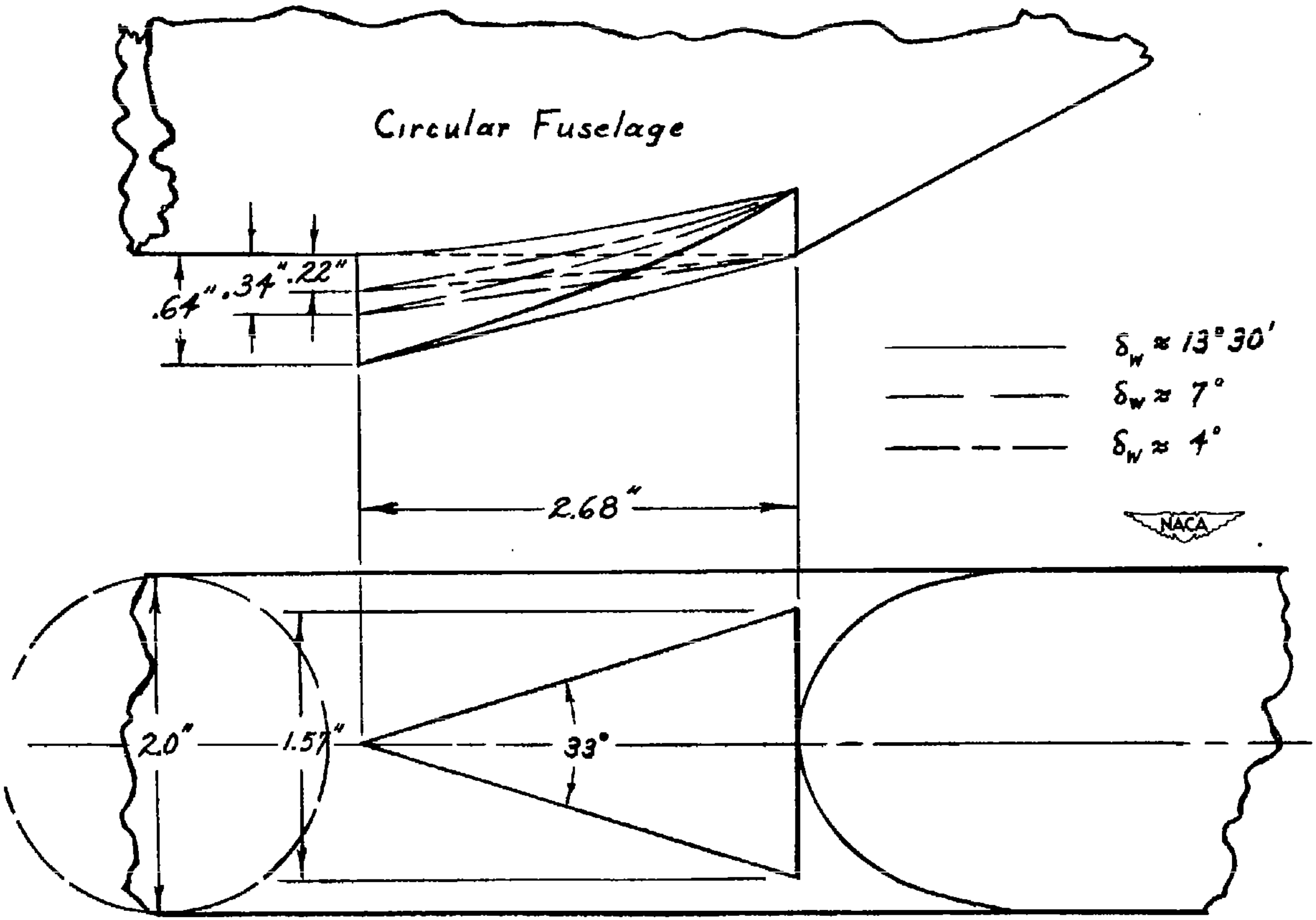

(b) For circular fuselage.

Figure 7.- Concluded.

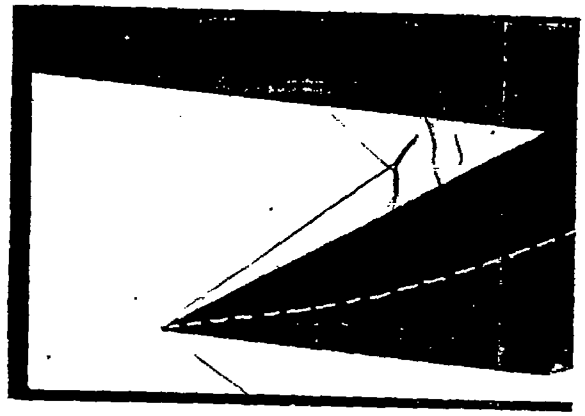

$\alpha = 5^{\circ}$

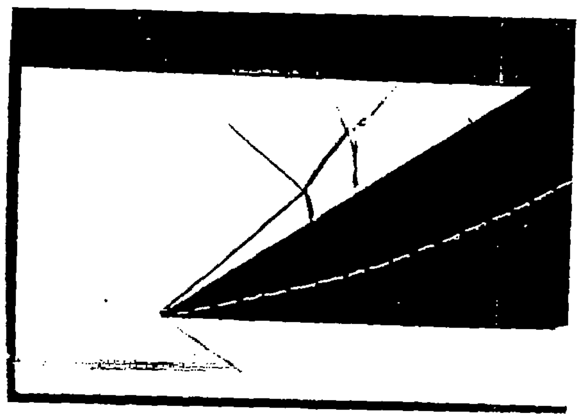

$\alpha = 0^{\circ}$

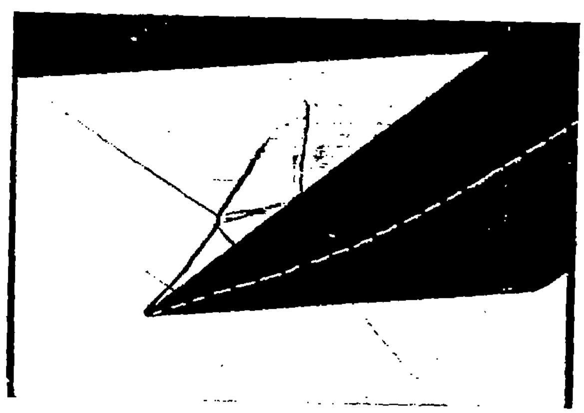

$\alpha = -5^{\circ}$

(a) $M_o = 2.03$.

L-76973

Figure 8.- Shadowgraphs of inlet with circular fuselage at various Mach numbers and angles of attack.

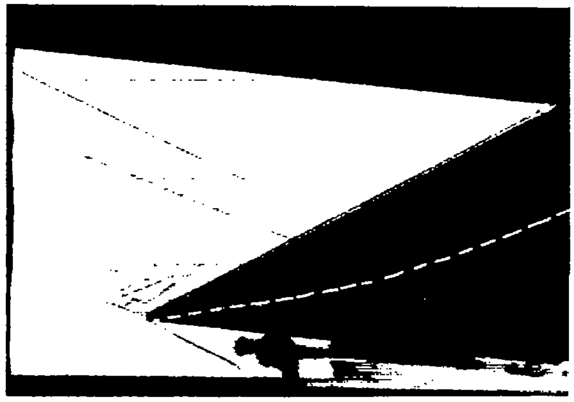

$\alpha = 5^{\circ}$

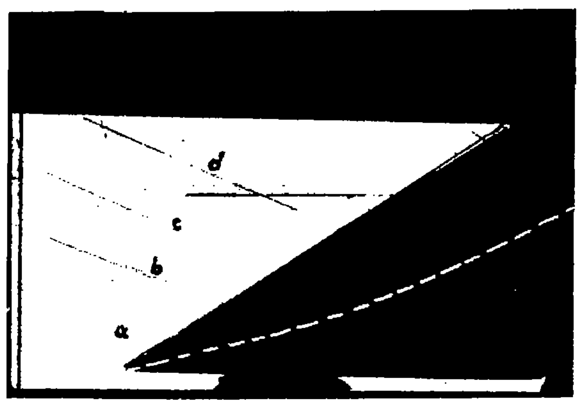

$\alpha = 0^{\circ}$

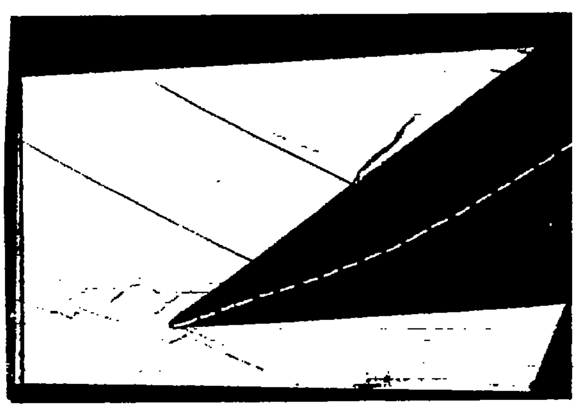

$\alpha = -5^{\circ}$

(b) $M_o = 2.71$.

NACA
L-76974

Figure 8.- Continued.

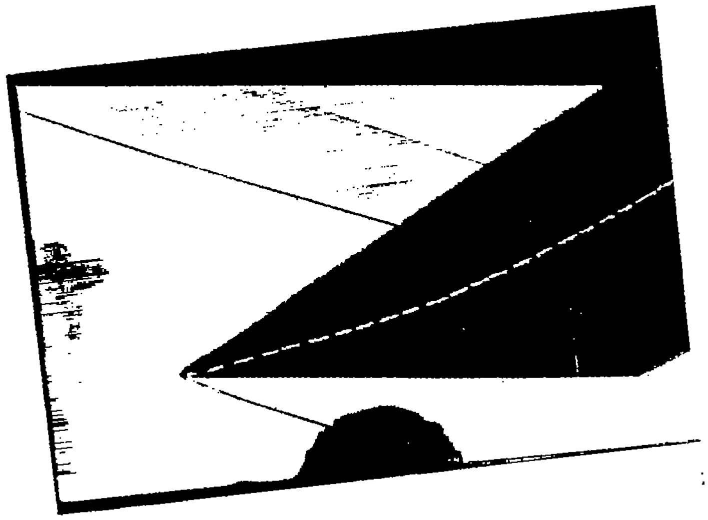

$\alpha = 5^{\circ}$

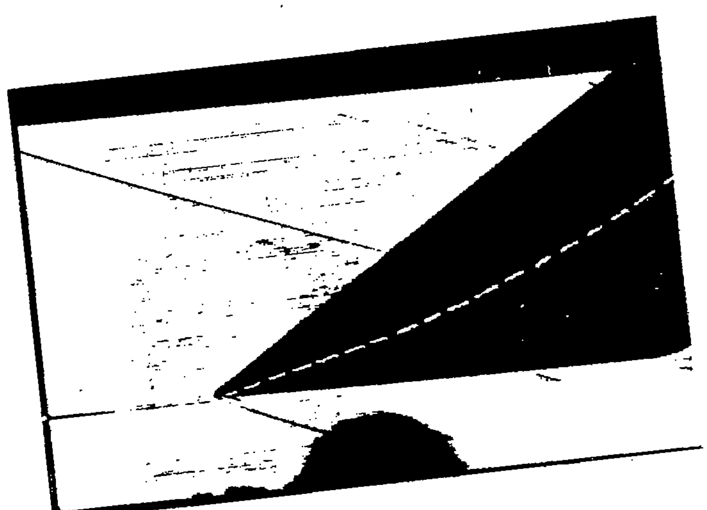

$\alpha = 0^{\circ}$

(c) $M_o = 3.12$.

NACA
L-76975

Figure 8.- Concluded.

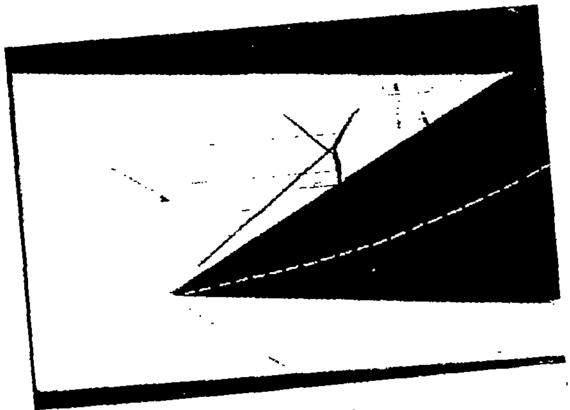

α = 5°

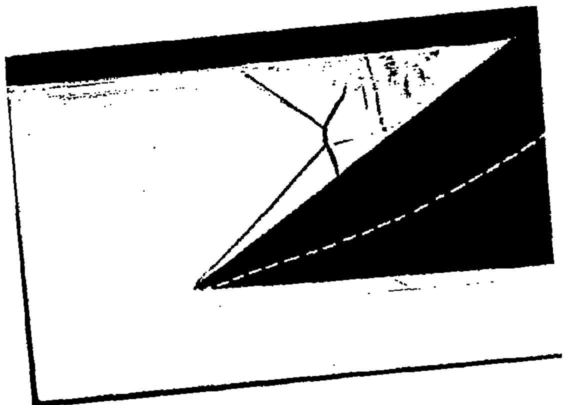

α = 0°

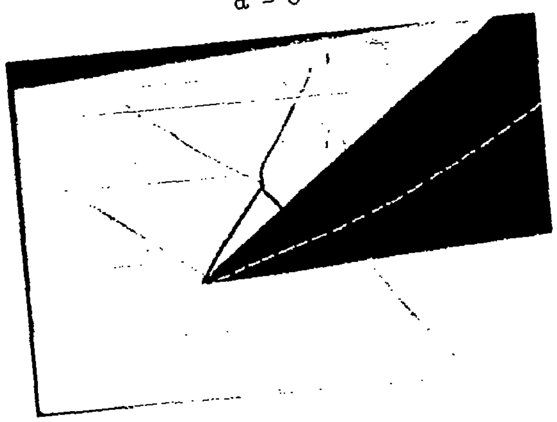

α = -5°

(a) $M_o = 2.03$.

L-76976

Figure 9.- Shadowgraphs of inlet with the rectangular fuselage in the flush condition and the bleed-off slot sealed at various Mach numbers and angles of attack.

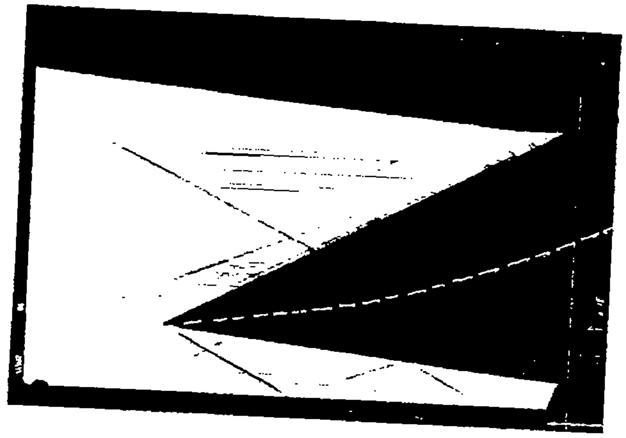

α = 5°

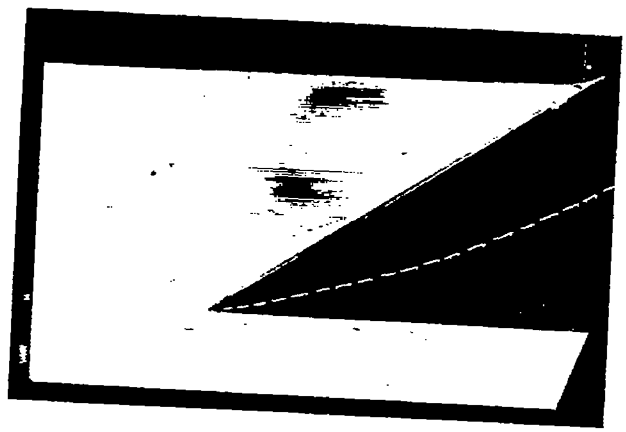

α = 0°

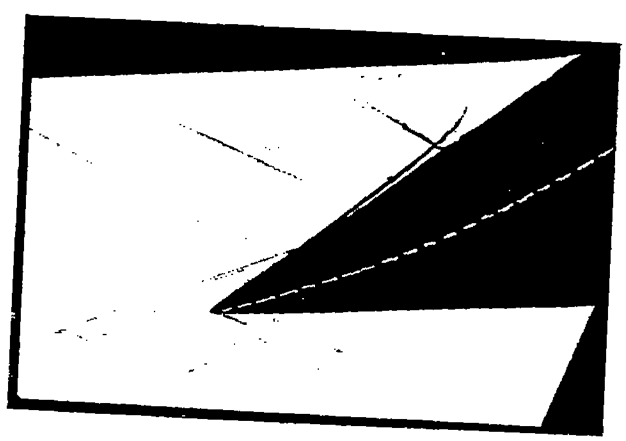

α = -5°

(b) $M_o = 2.71$.

Figure 9.- Concluded. L-76977

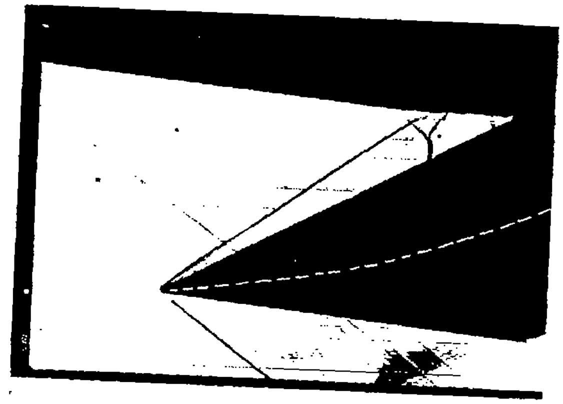

$\alpha = 5^{\circ}$

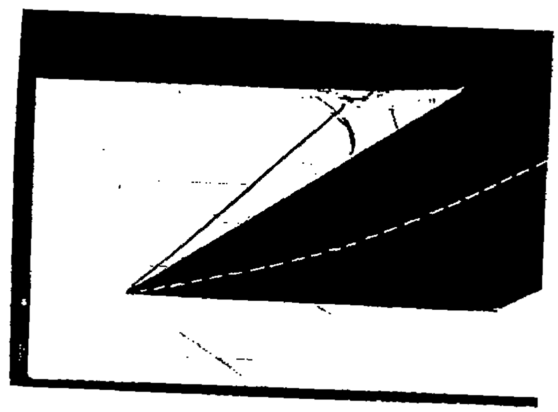

$\alpha = 0^{\circ}$

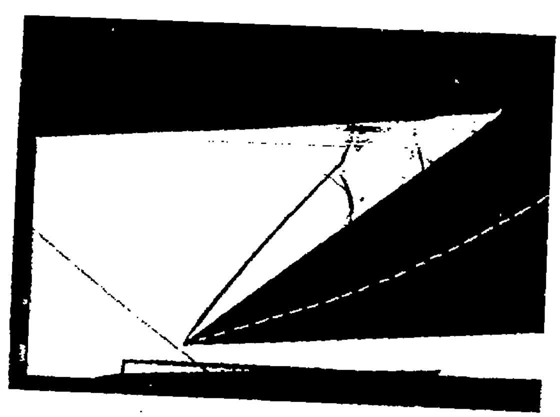

$\alpha = -5^{\circ}$

(a) M = 2.03.

L-76978

Figure 10.- Shadowgraphs of inlet with the rectangular fuselage in the flush condition, bleed-off slot open and suction applied at various Mach numbers and angles of attack.

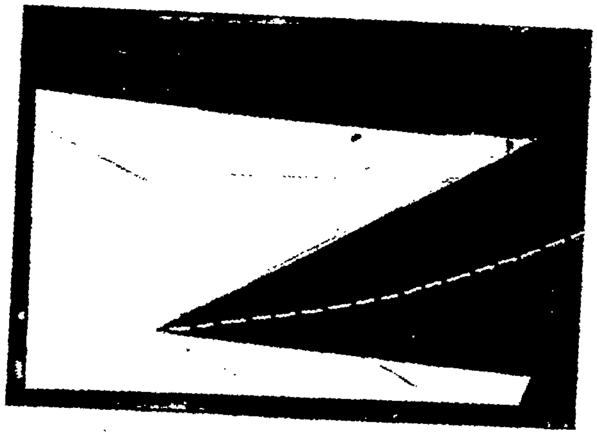

$\alpha = -5^{\circ}$

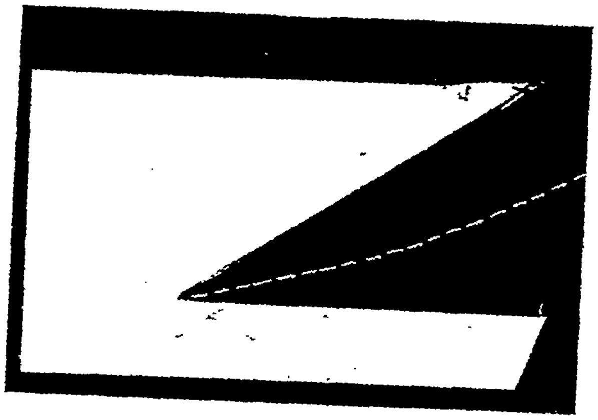

$\alpha = 0^{\circ}$

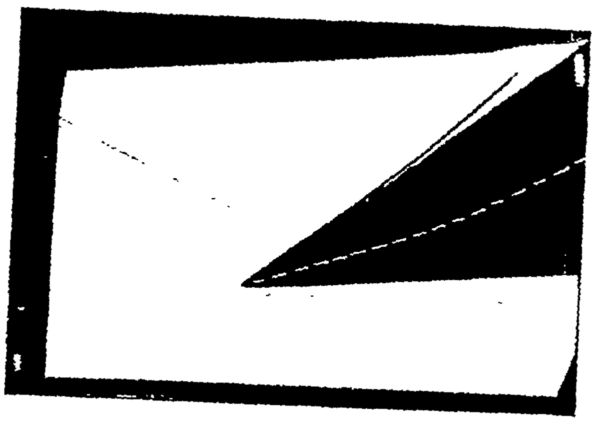

$\alpha = 5^{\circ}$

(b) $M_o = 2.71$.

Figure 10.- Concluded.

L-76979

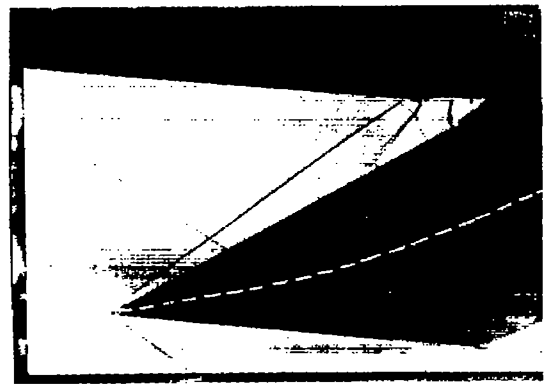

$\alpha = -5^{\circ}$

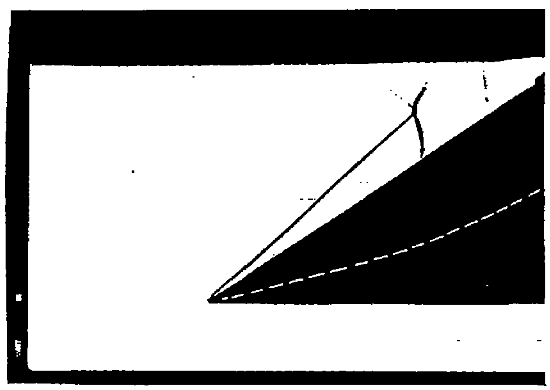

$\alpha = 0^{\circ}$

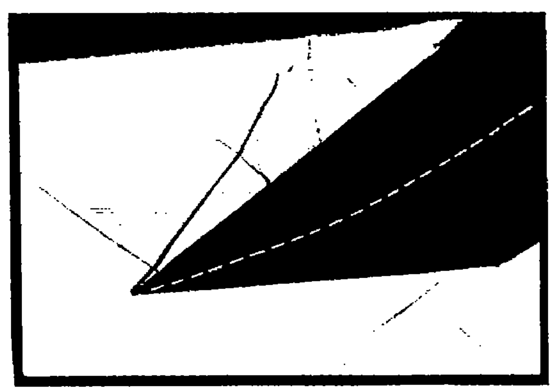

$\alpha = 5^{\circ}$

(a) $M_o = 2.03$.

NACA
L-76980

Figure 11.- Shadowgraphs of inlet with the rectangular fuselage in the offset condition and the bleed-off slot exit open to atmospheric pressure at various Mach numbers and angles of attack.

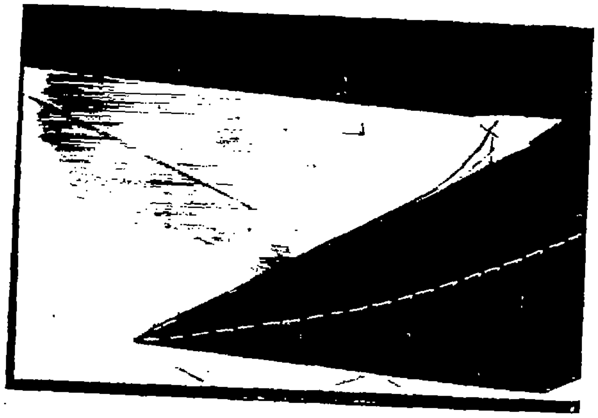

$\alpha = -5^{\circ}$

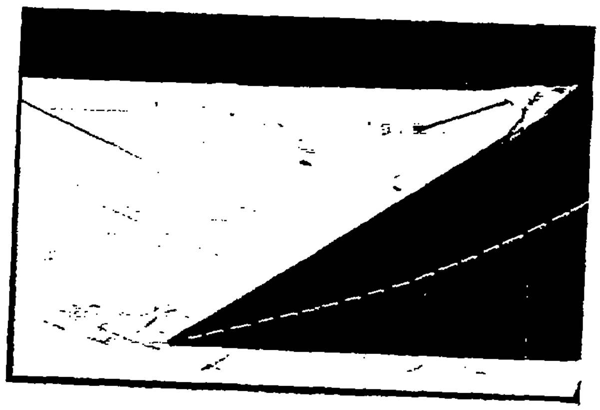

$\alpha = 0^{\circ}$

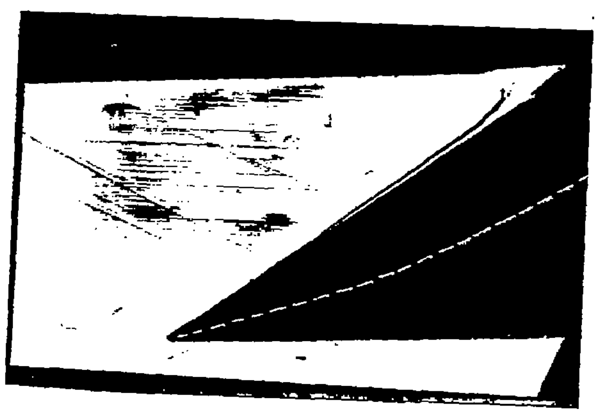

$\alpha = 5^{\circ}$

(b) $M_o = 2.71$.

Figure 11.- Concluded.

NACA
L-76981

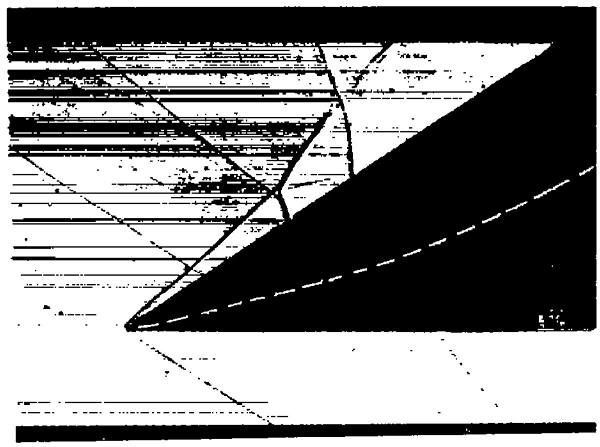

$\delta_w = 0^\circ$

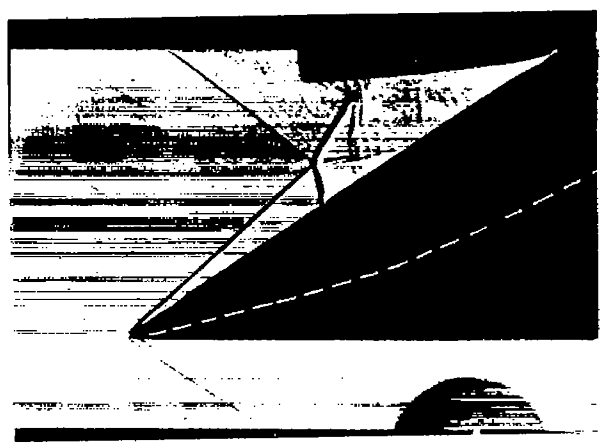

$\delta_w = 7^\circ$

NACA
L-76982

Figure 12.- Shadowgraphs of inlet with the circular fuselage for two wedge deflections. $\alpha = 0^\circ$; $M_0 = 2.03$.

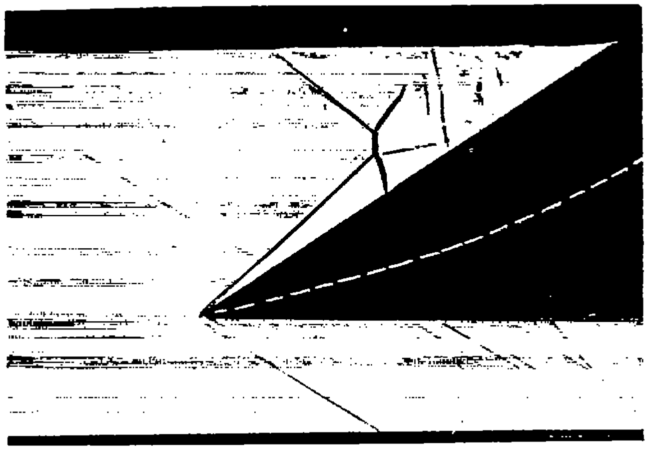

$\delta_w = 0^\circ$

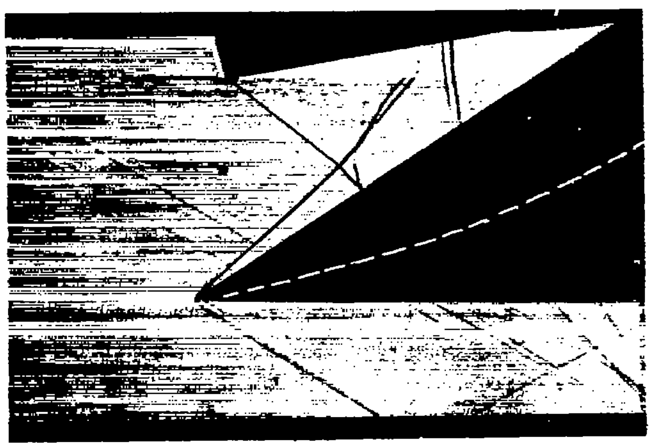

$\delta_w = 9^\circ$

NACA
L-76983

Figure 13.- Shadowgraphs of inlet with the rectangular fuselage in the flush condition and the bleed-off slot sealed for two wedge deflections. $\alpha = 0^\circ$; $M_o = 2.03$.

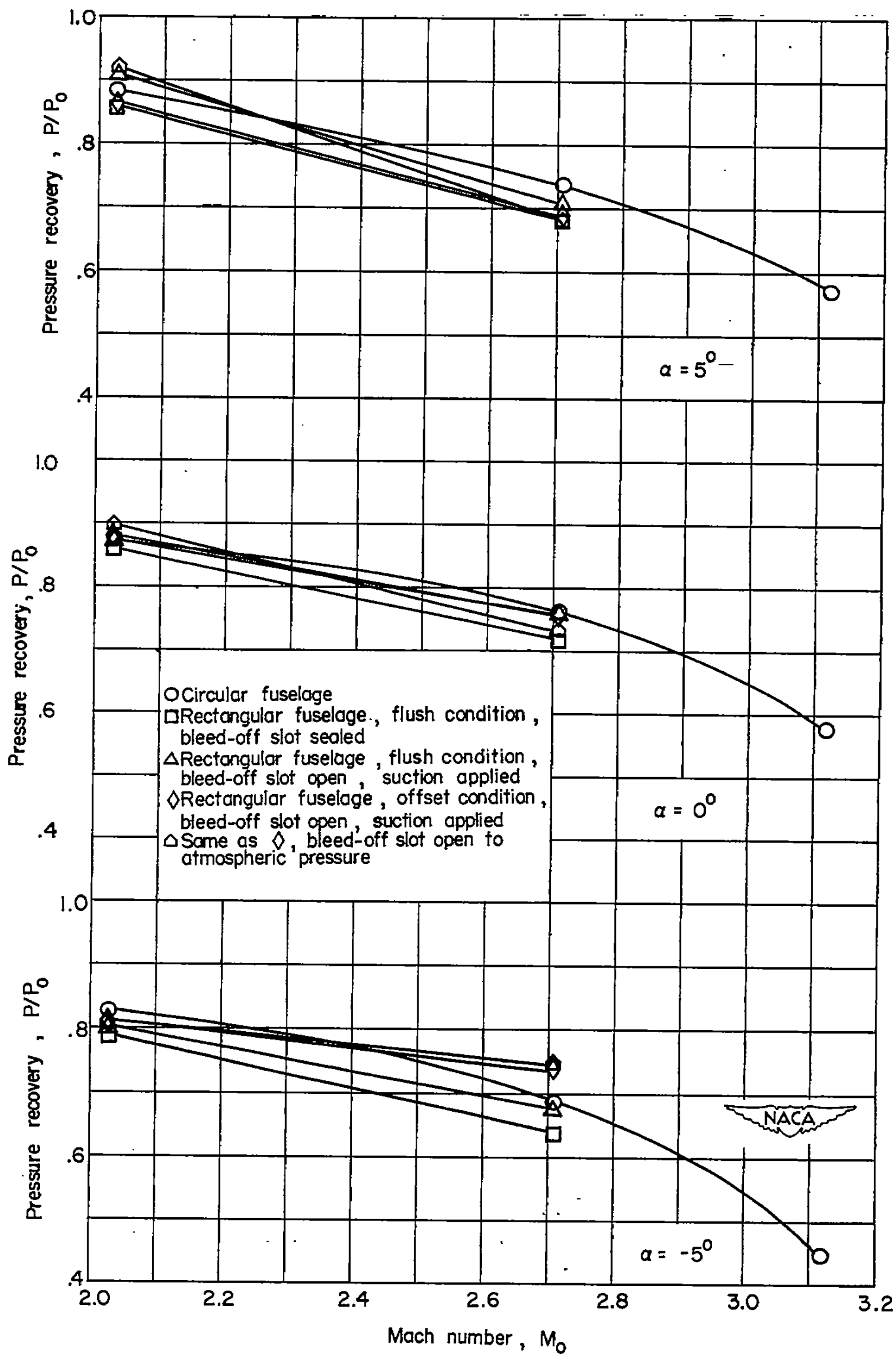

Figure 14.- Variation of maximum pressure recovery with Mach number for a supersonic, swept, rectangular scoop inlet. $\delta_w = 0^\circ$.

[redacted]

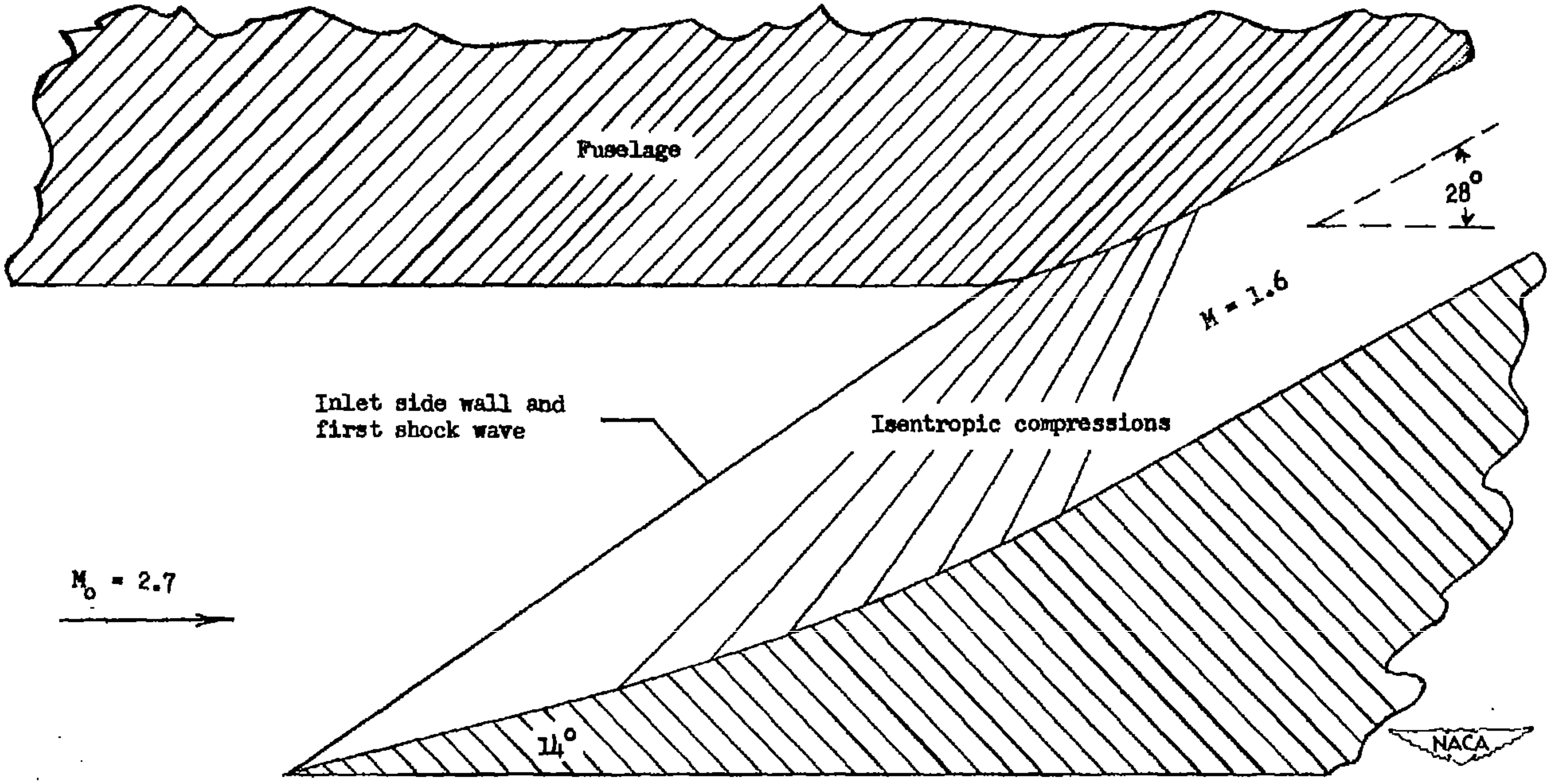

Figure 15.- Proposed modification of design flow pattern for swept, rectangular scoop inlet.

[redacted]

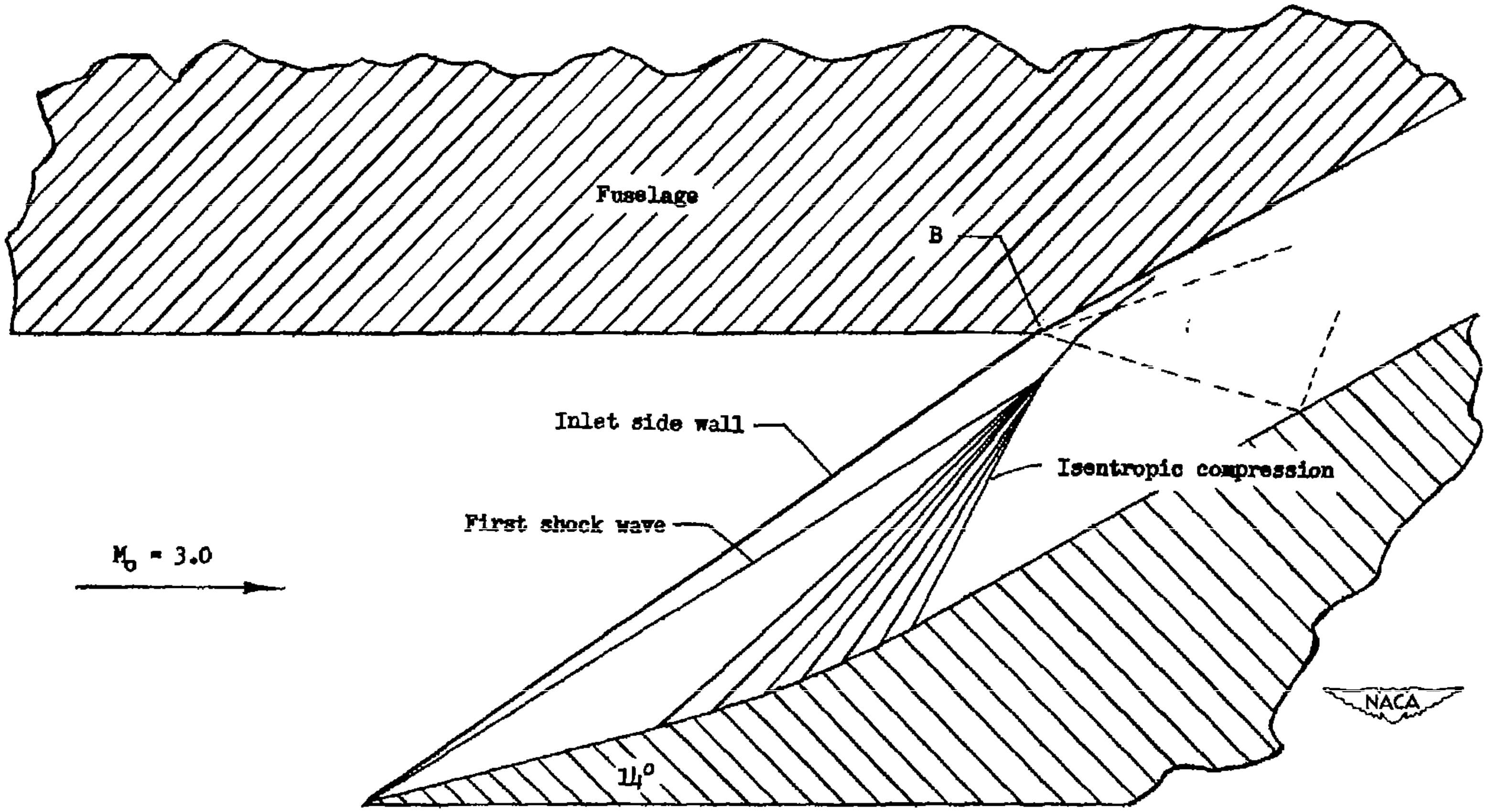

Figure 16.- Theoretical flow pattern at $M_0 = 3.0$ for a supersonic, swept, rectangular scoop inlet designed for $M_0 = 2.7$.

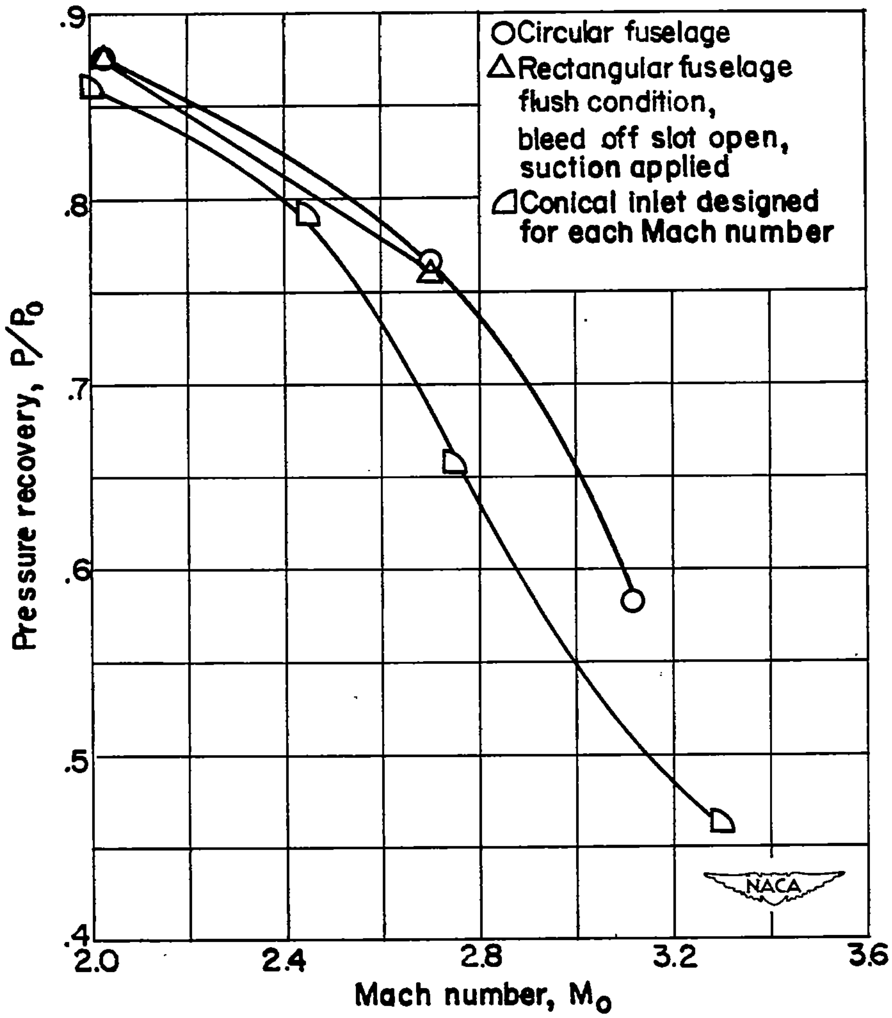

Figure 17.- Variation of maximum pressure recovery with Mach number for a supersonic, swept, rectangular scoop inlet designed for $M_0 = 2.7$ compared to conical inlets (refs. 2 and 5) designed for each Mach number indicated. $\alpha = 0^{\circ}$.

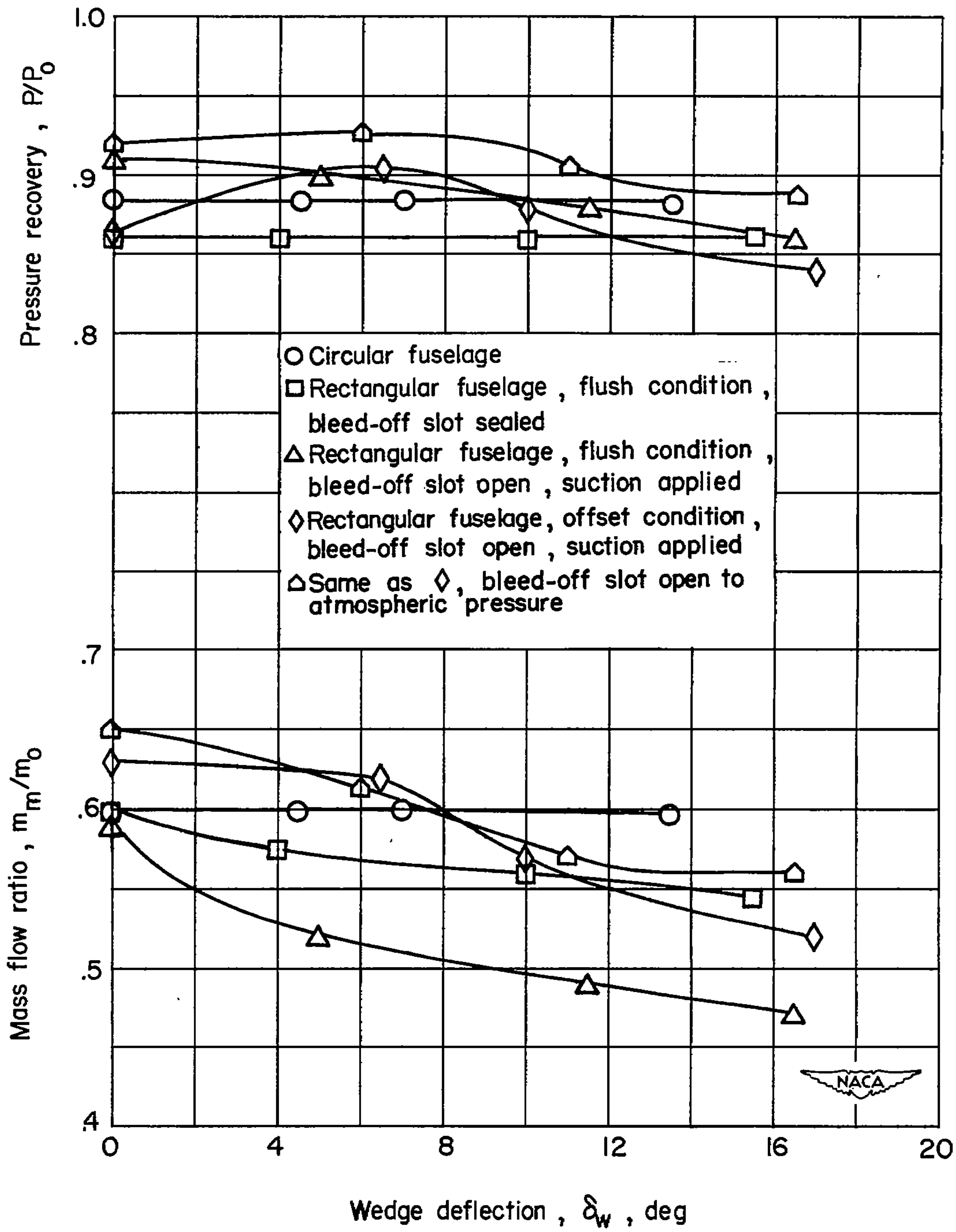

(a) $\alpha = 5^{\circ}$.

Figure 18.- Effect of wedge deflection on the maximum pressure recovery and mass-flow ratio of a supersonic, swept, rectangular scoop inlet. $M_o = 2.03$.

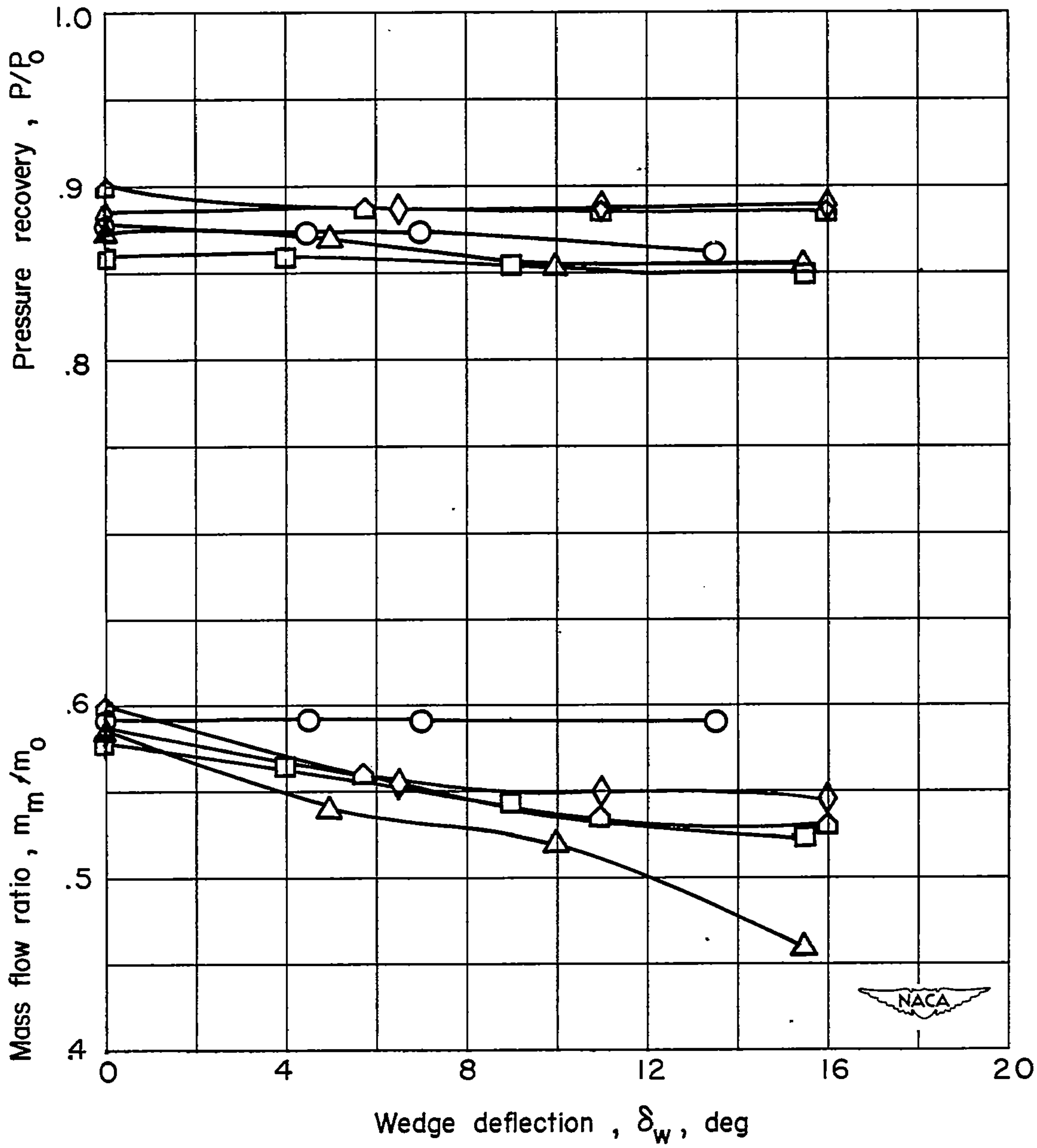

(b) $\alpha = 0^{\circ}$.

Figure 18.- Continued.

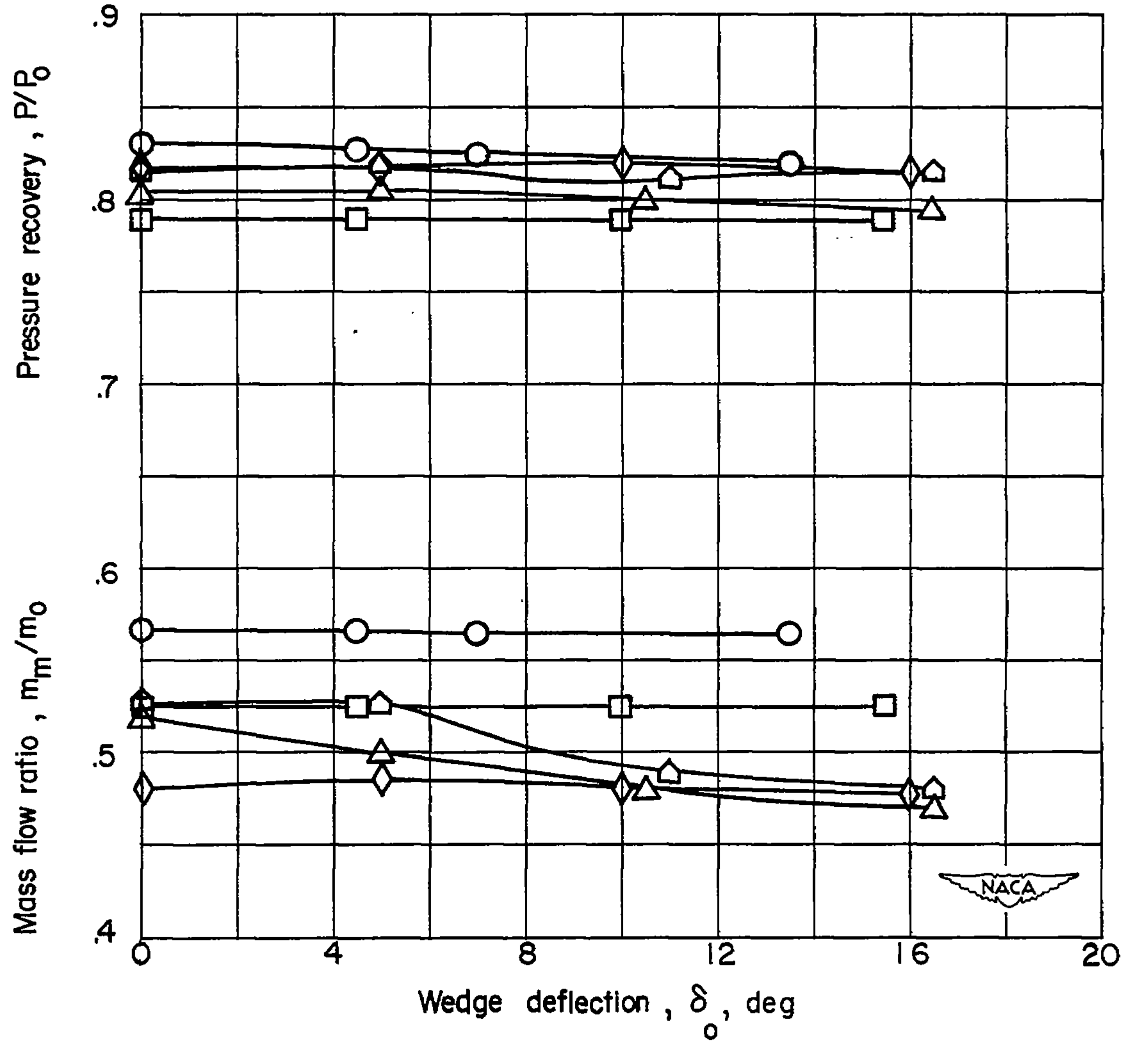

(c) $\alpha = -5^{\circ}$.

Figure 18.- Concluded.

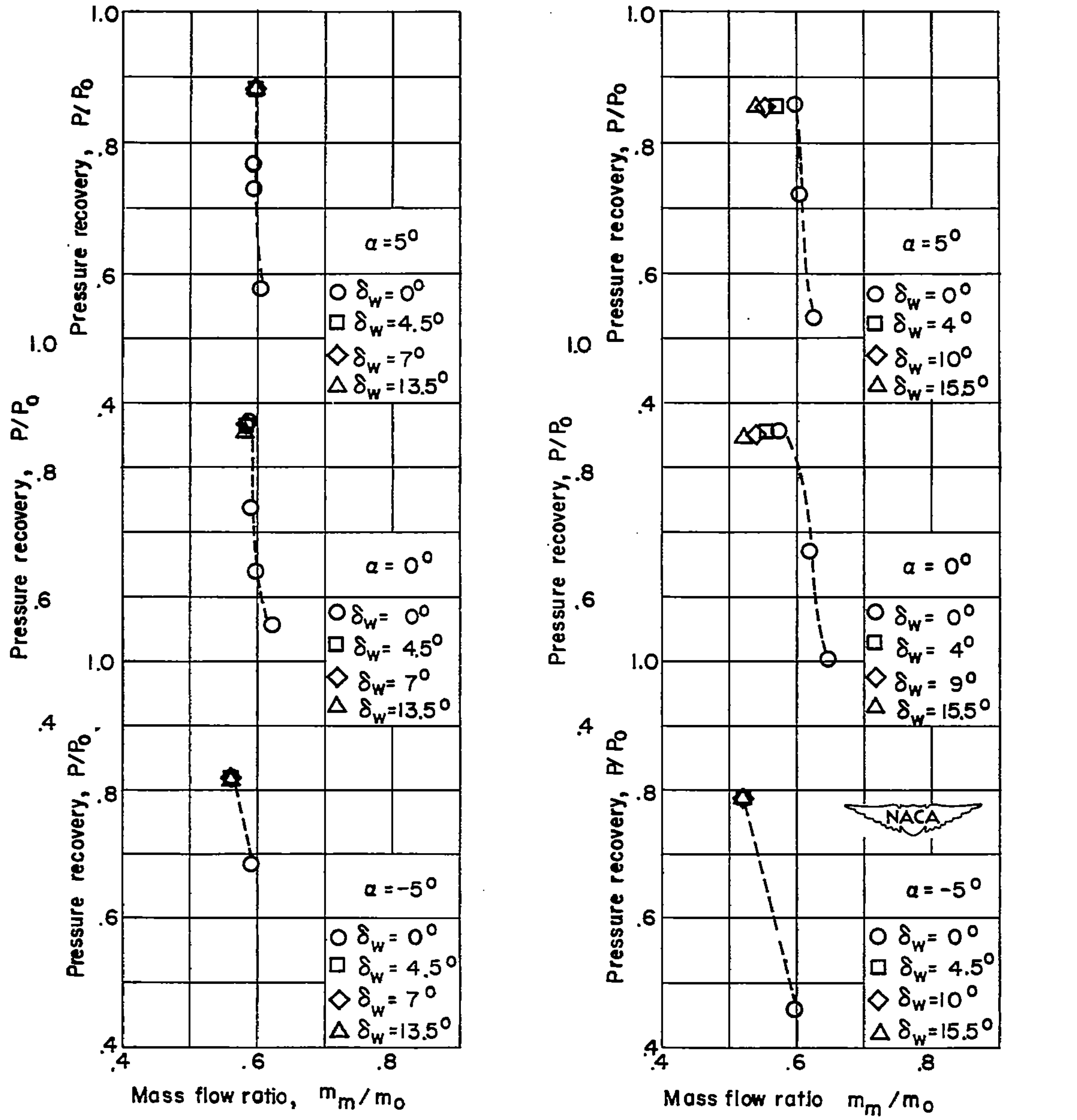

(a) Circular fuselage

(b) Rectangular fuselage flush condition, bleed-off slot sealed

Figure 19.- Variation of pressure recovery with mass-flow ratio for various wedge deflections and angles of attack. $M_o = 2.03$.

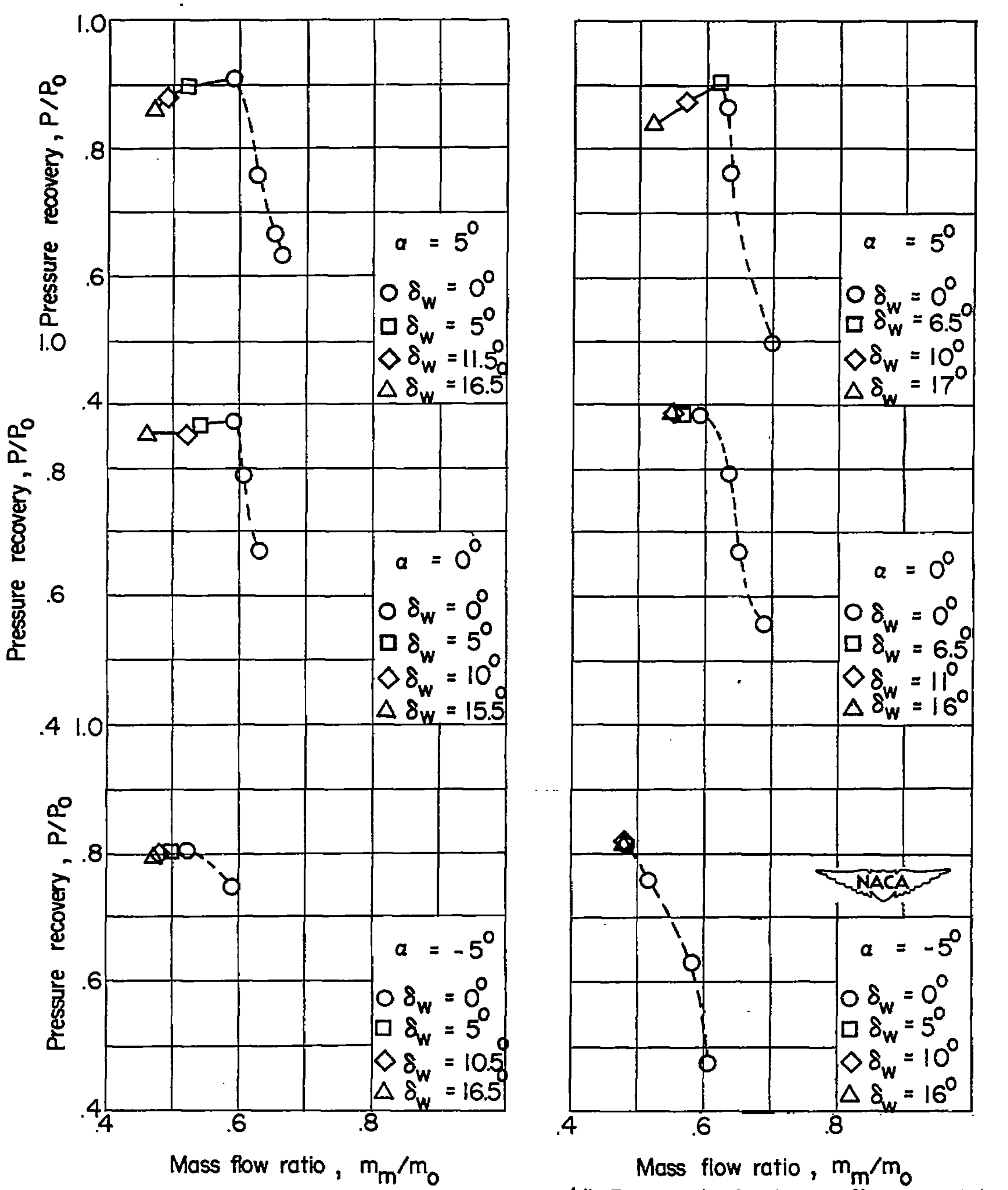

(c) Rectangular fuselage, flush condition, bleed-off slot open, suction applied.

(d) Rectangular fuselage, off-set condition, bleed-off slot open, suction applied.

Figure 19.- Continued.

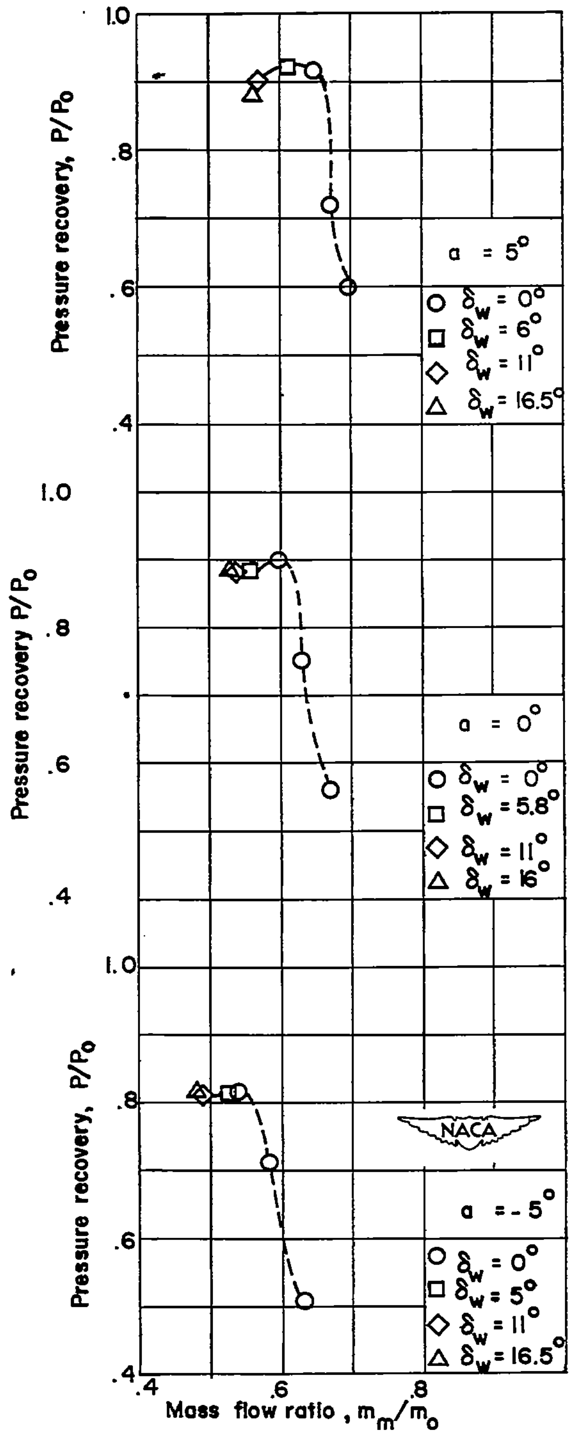

(e) Rectangular fuselage, offset condition, bleed-off slot open to atmospheric pressure

Figure 19.- Concluded.

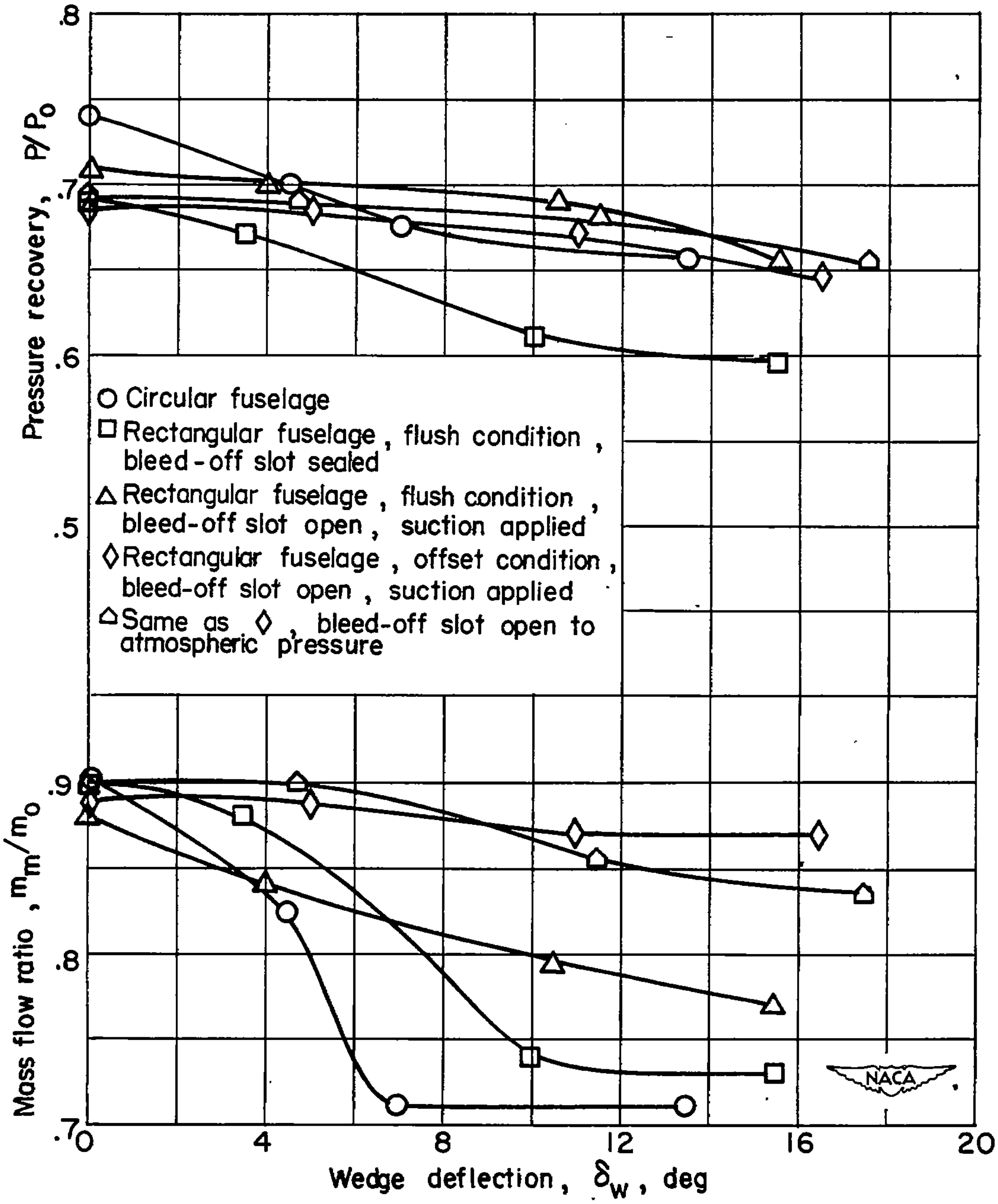

(a) $\alpha = 5^{\circ}$.

Figure 20.- Effect of wedge deflection on the maximum pressure recovery and mass-flow ratio of a supersonic, swept, rectangular scoop inlet. $M_o = 2.71$.

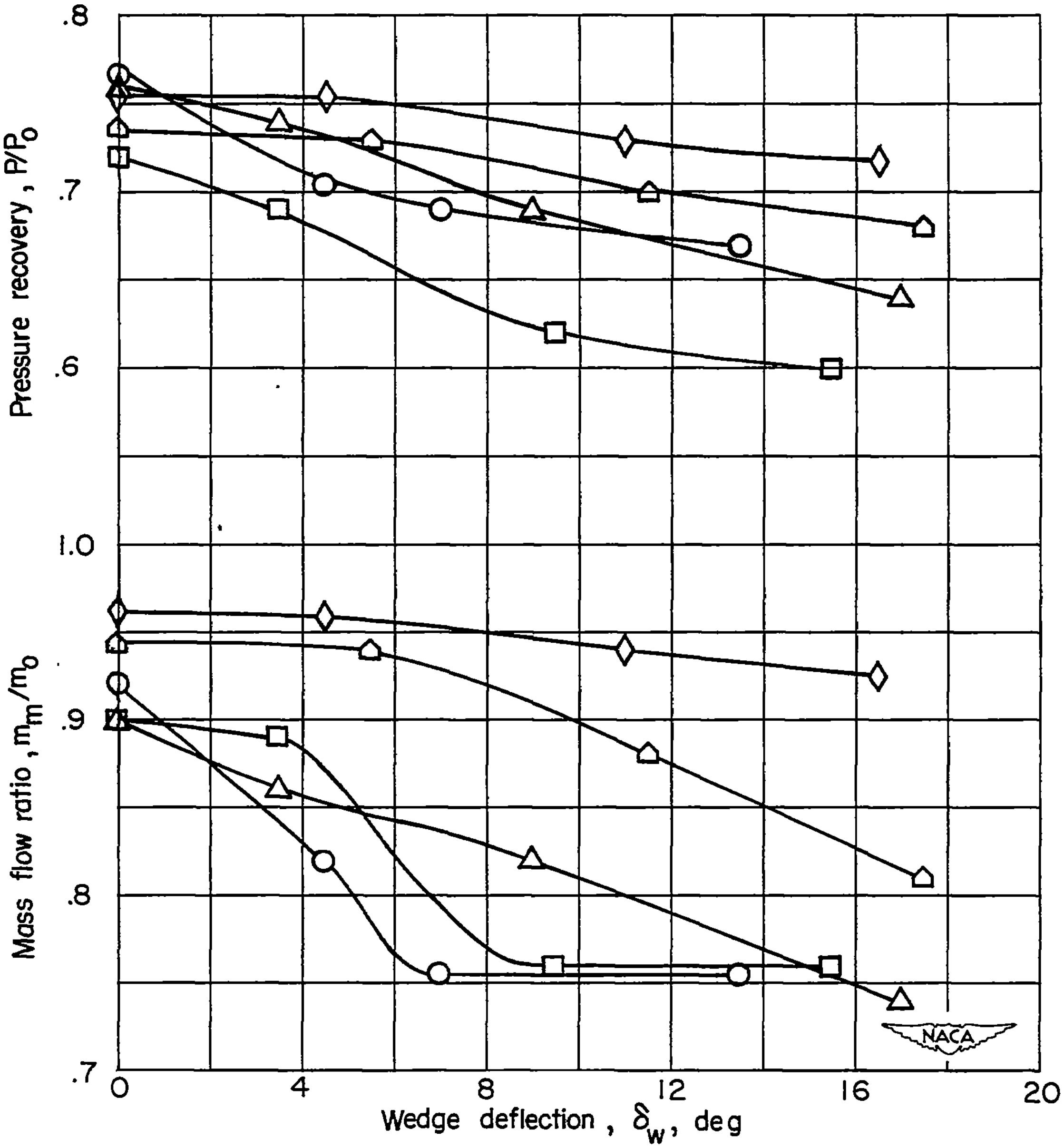

(b) $\alpha = 0^{\circ}$.

Figure 20.- Continued.

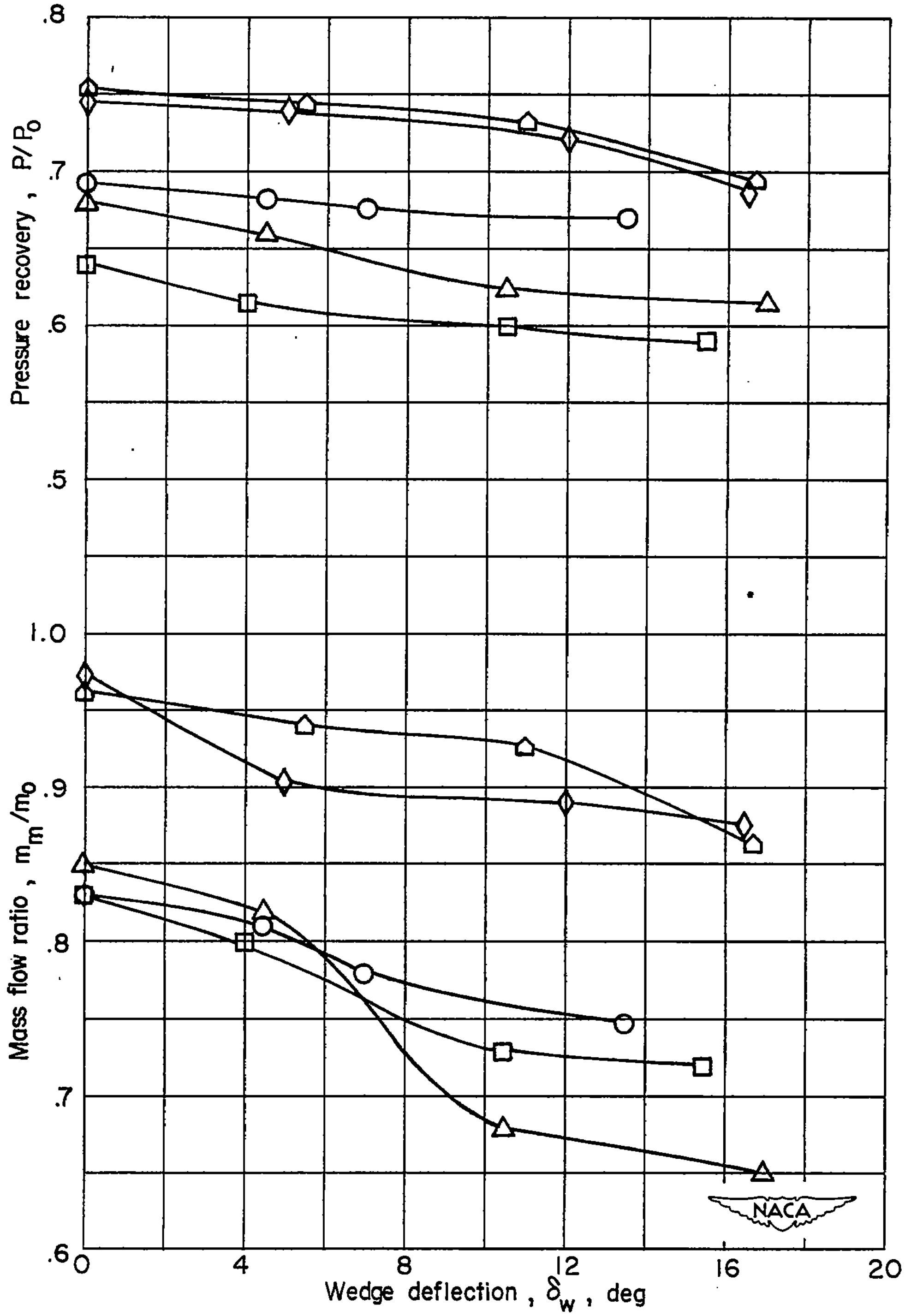

(c) $\alpha = -5^{\circ}$.

Figure 20.- Concluded.

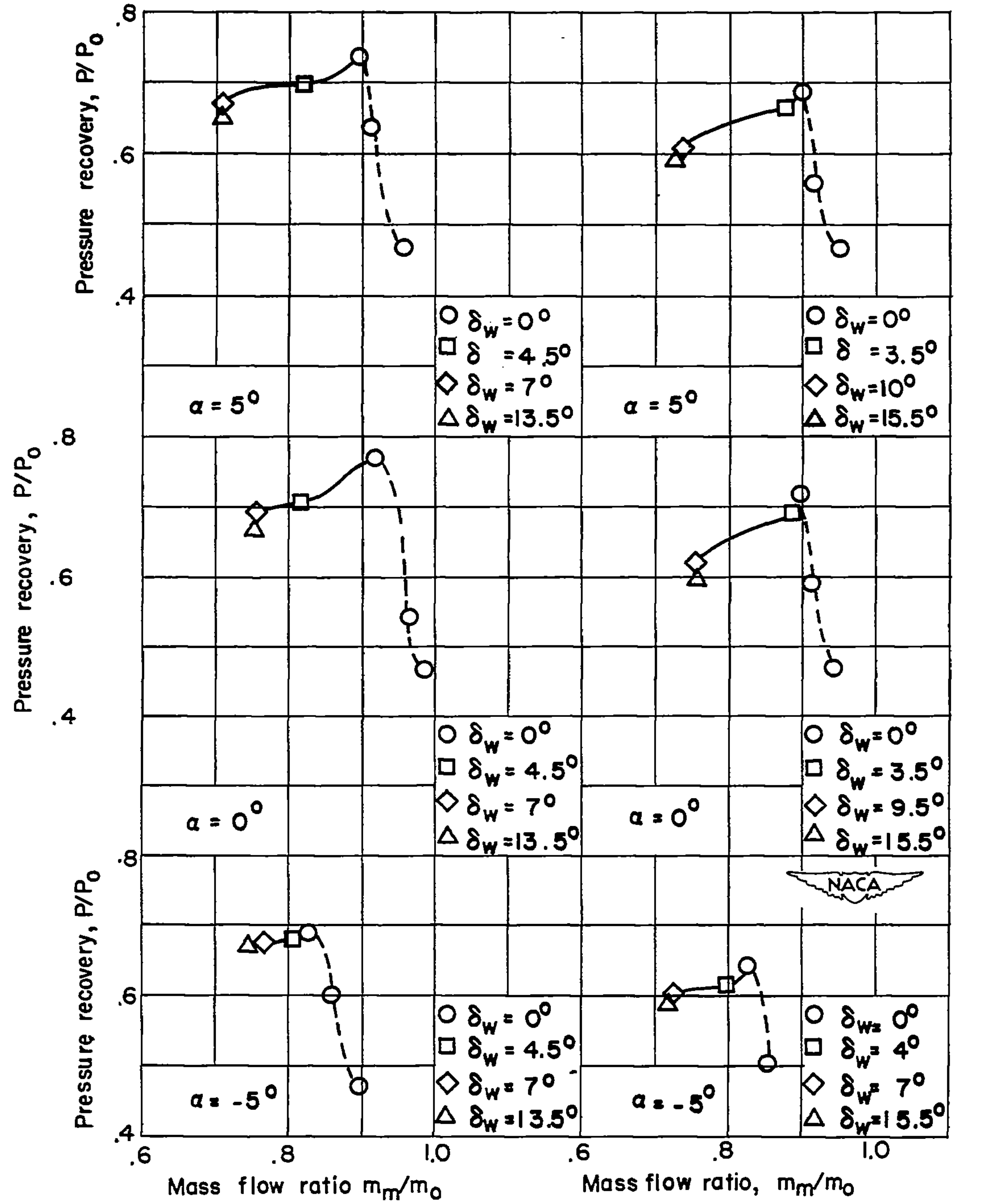

(a) Circular fuselage.

(b) Rectangular fuselage, flush condition, bleed off slot sealed.

Figure 21.- Variation of pressure recovery with mass-flow ratio for various wedge deflections and angles of attack. M_0 = 2.71.

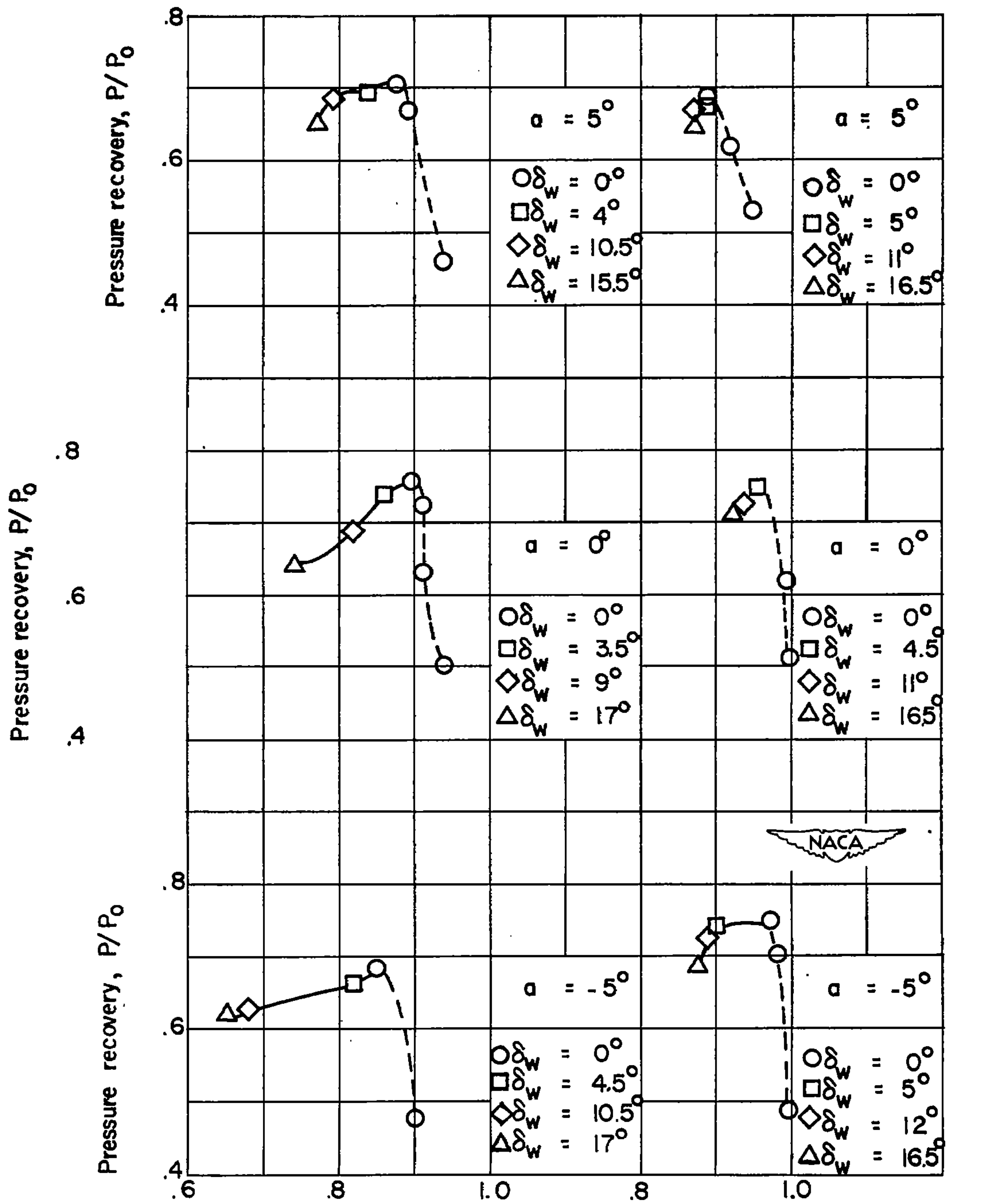

(c) Rectangular fuselage, flush condition, bleed-off slot open, suction applied

(d) Rectangular fuselage, offset condition, bleed-off slot open, suction applied.

Figure 21.- Continued.

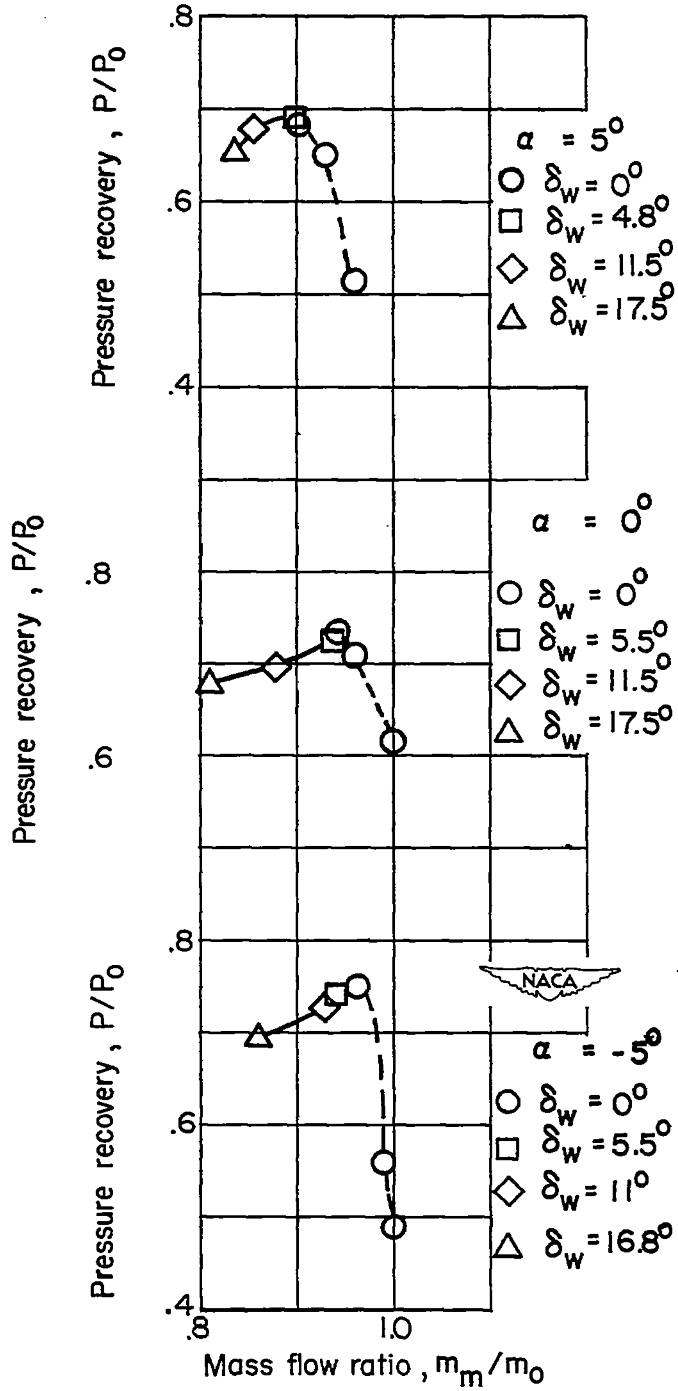

(e) Rectangular fuselage, offset condition, bleed-off slot open to atmospheric pressure.

Figure 21.- Concluded.

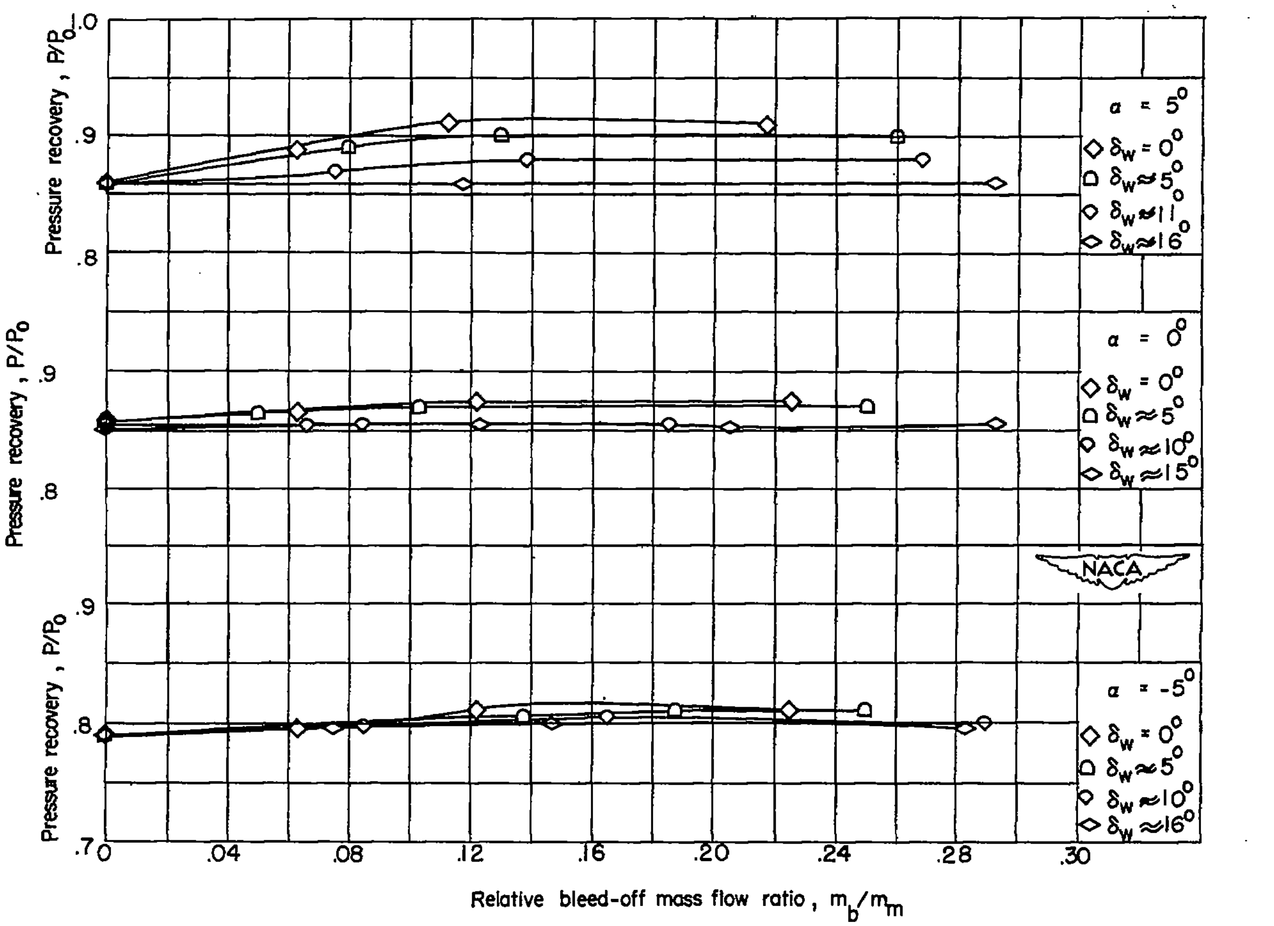

(a) $M_0 = 2.03$.

Figure 22.- Effect of relative mass-flow ratio through the bleed-off slot on the maximum pressure recovery of the rectangular fuselage, flush condition, for various wedge deflections and angles of attack.

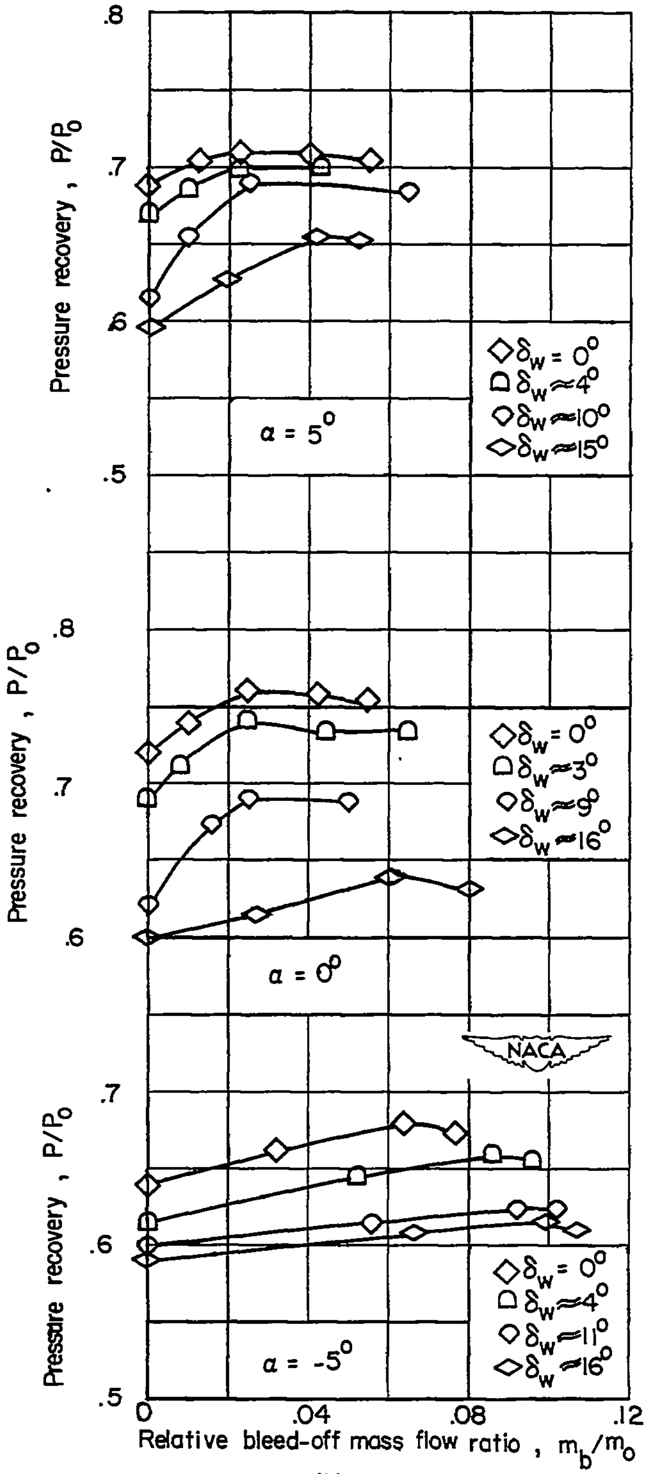

(b) M_o = 2.71.

Figure 22.- Concluded.

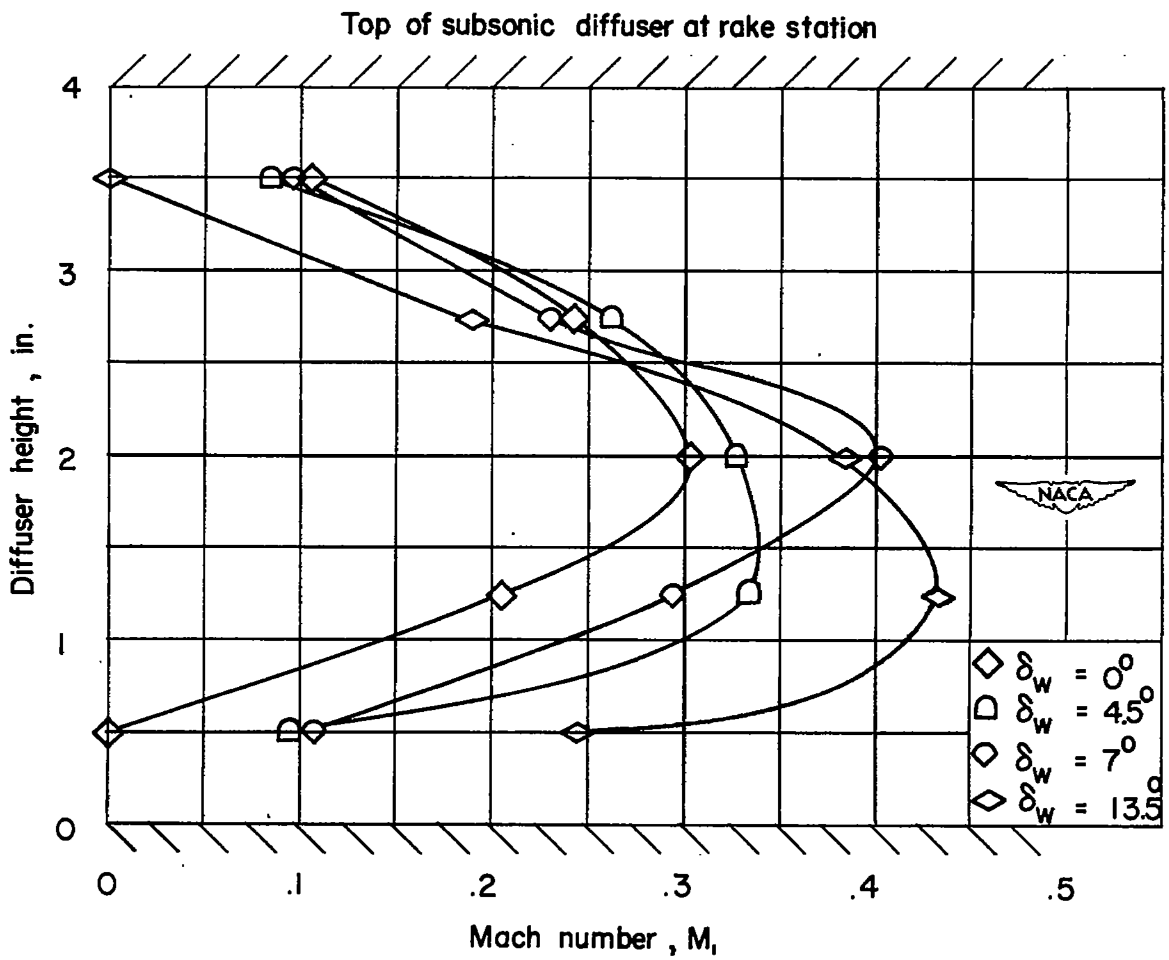

(a) Circular fuselage.

Figure 23.- Mach number distribution at the rake station in the subsonic diffuser. $\alpha = 0^\circ$; $M_o = 2.03$.

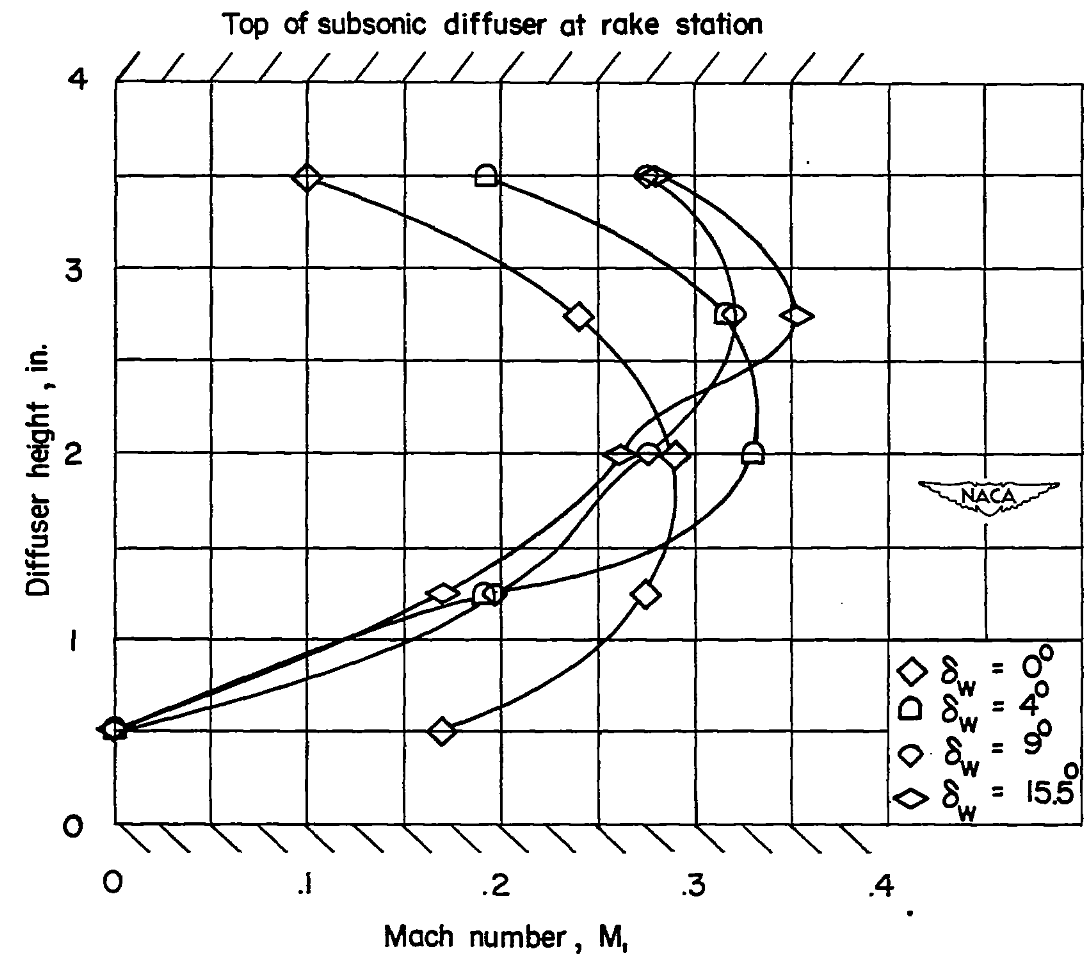

(b) Rectangular fuselage, flush condition, bleed-off slot sealed.

Figure 23.- Continued.

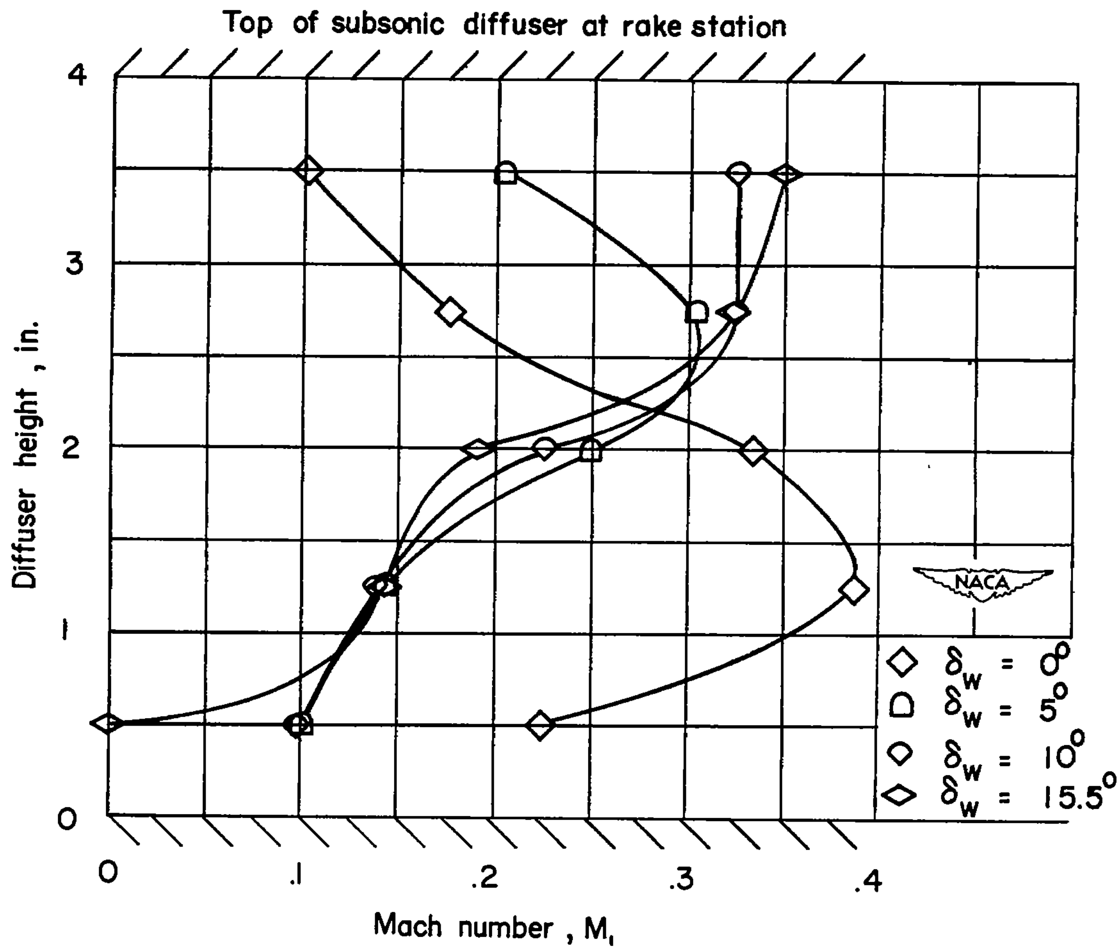

(c) Rectangular fuselage, flush condition, bleed-off slot open, suction applied.

Figure 23.- Concluded.

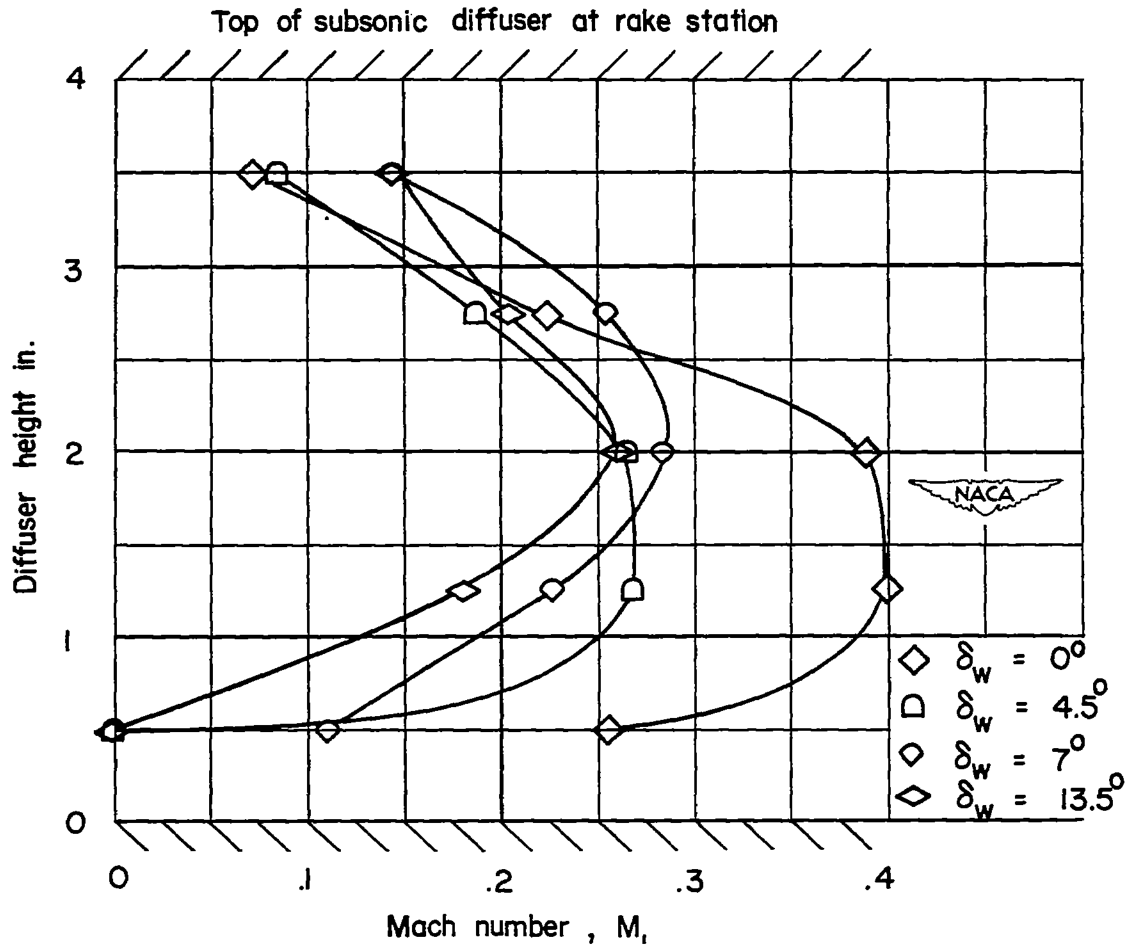

(a) Circular fuselage.

Figure 24.- Mach number distribution at the rake station in the subsonic diffuser. $\alpha = 0^\circ$; $M_0 = 2.71$.

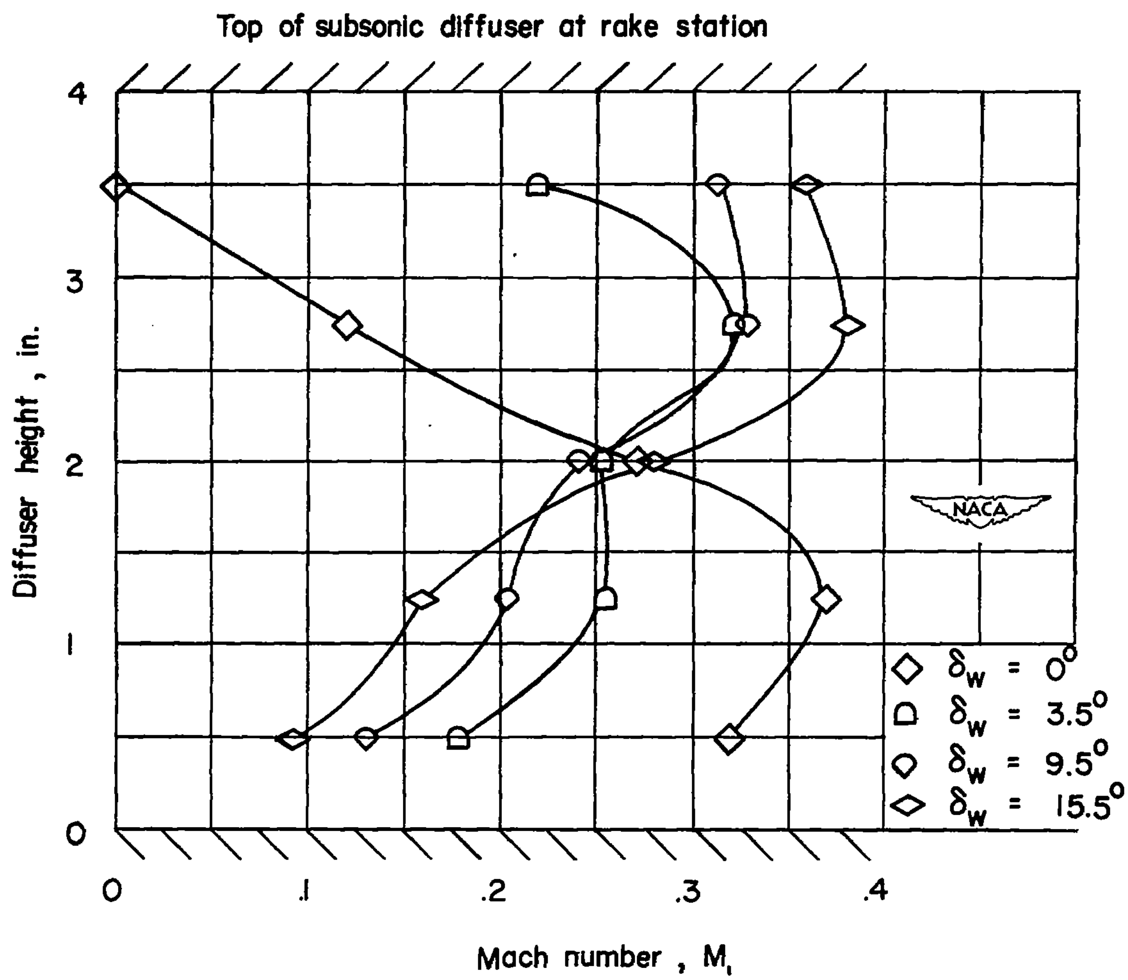

(b) Rectangular fuselage, flush condition,
bleed-off slot sealed.

Figure 24.- Continued.

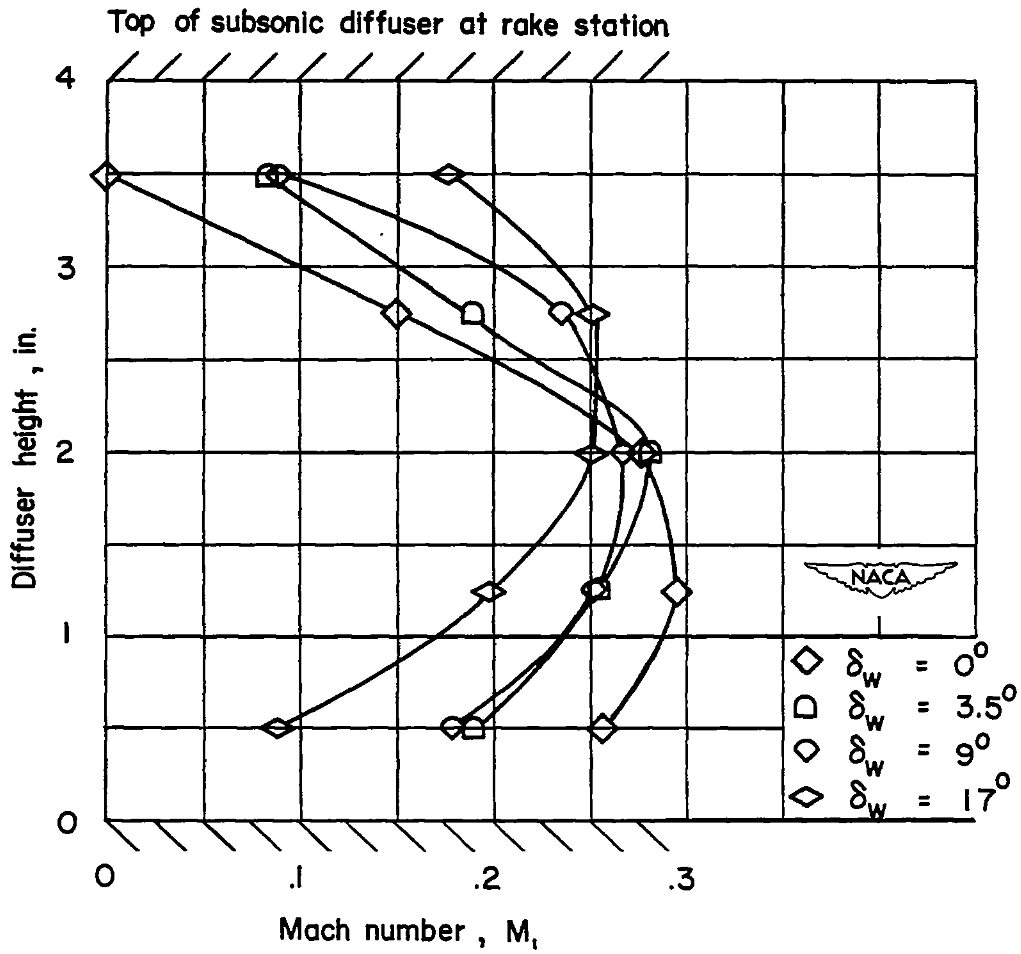

(c) Rectangular fuselage, flush condition, bleed-off slot open, suction applied.

Figure 24.- Concluded.

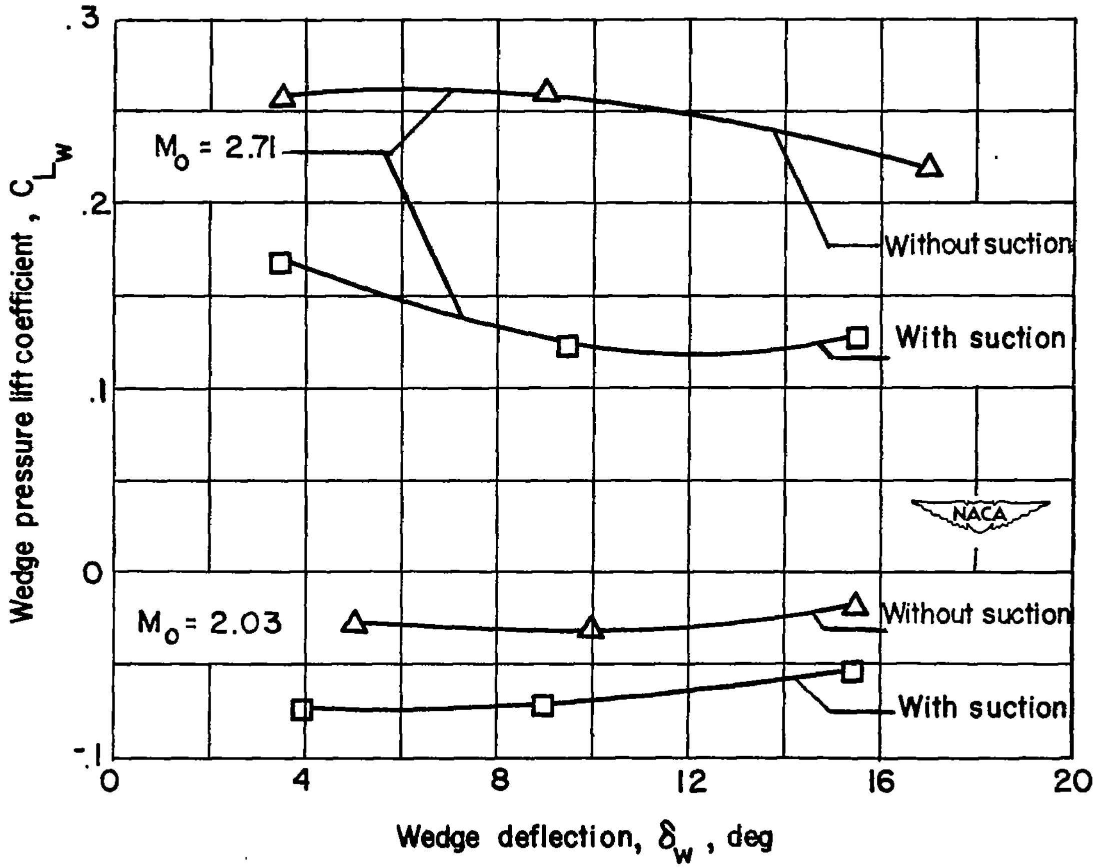

Figure 25.- Effect of wedge deflection on wedge lift coefficient, rectangular fuselage, flush condition. $\alpha = 0^{\circ}$.

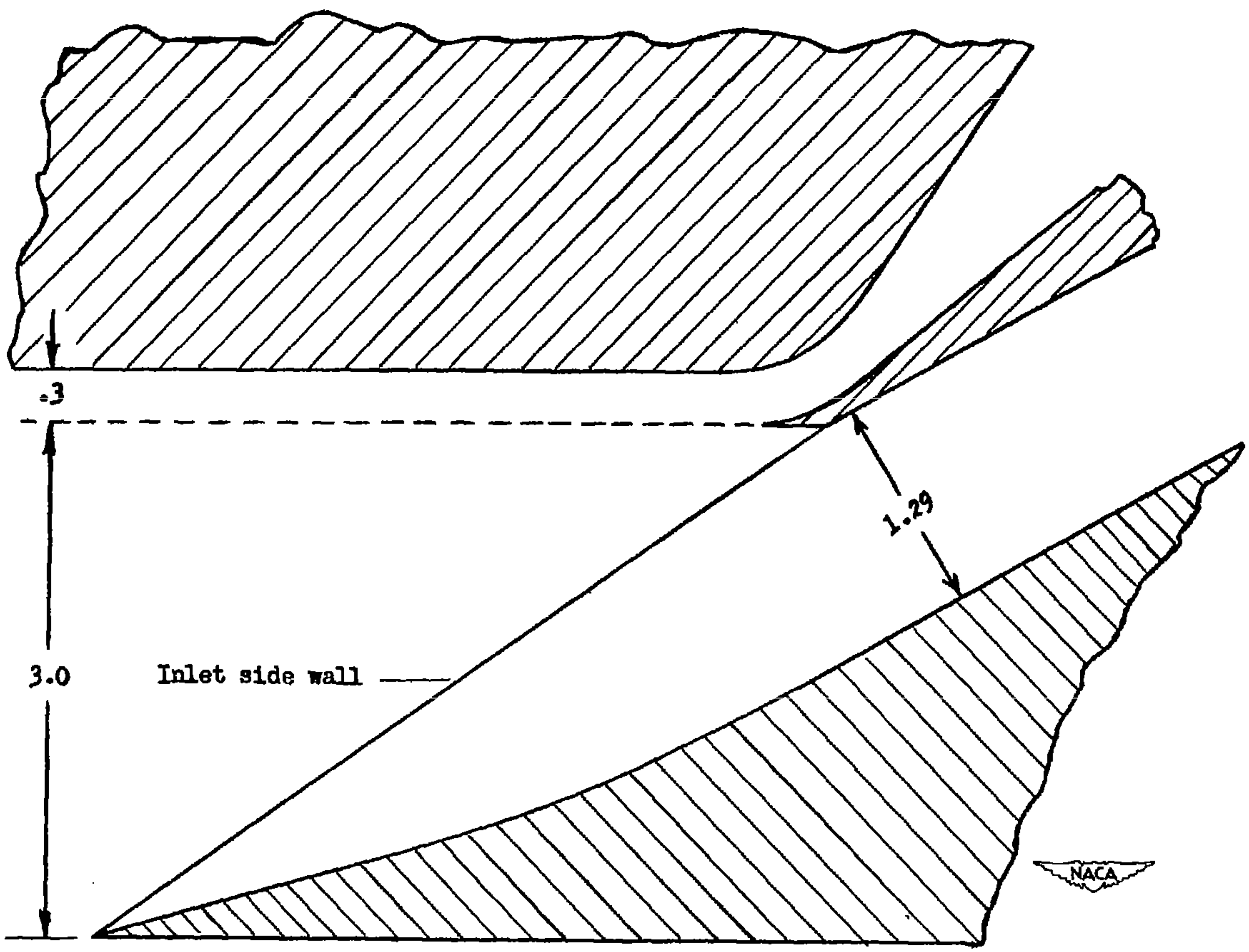

Figure 26.- Proposed modification of inlet to aid starting.

NACA-Langley - 11-26-52 - 350